Analysis of Indoor Radon in Texas and Depleted Uranium in Hawai'i

By

Lucy Lim, BSc/MSc

A Dissertation

In

Environmental Toxicology

Submitted to the Graduate Faculty
of Texas Tech University, in
Partial Fulfillment of
the Requirements for
the Degree of

DOCTOR OF PHILOSOPHY

Approved

David M. Klein
Chair of Committee

Todd Anderson

Callum Hetherington

Guofeng Cao

Mark Sheridan
Dean of the Graduate School

May 2019

ACKNOWLEDGEMENTS

I would like to thank Texas Tech University, The Institute of Environment and Human Health, for providing research assistantship through the Environmental Protection Agency (EPA) Indoor Radon Grant. Mr. George Brozowski, EPA Region 6 Health Physicist/Senior Radon Policy Advisor, for his trust in my ability to educate Texans on indoor radon. Thanks to the Kaho'olawe Island Reserve Commission which granted permission to acquire soil samples on Kaho'olawe Island. I also am grateful to my committee for writing support; TIEHH professors who taught with a passion and gladly spent extra time to answer classroom questions; TIEHH administrative staff who eagerly provided continuous guidance and direction for graduation and everyday life events.

Lastly, and most importantly, I would like to thank my spouse and sons (BJ and KC) for the endless encouragement that sustained me over the years to fulfill my dream of earning a Ph.D. Through them, and the sustaining grace of God, I can prepare for my next journey.

LIST OF TABLES

LIST OF FIGURES

PREFACE

This dissertation is composed of three topics related to mass spectrometry and environmental uranium. Each was written as separate chapters and formatted as manuscripts for publication to three different peer review journals. Chapter I is a published review of Fourier Transform Mass Spectrometry. Chapter II discusses the investigation of potential depleted uranium (DU) release from radiation control/impact areas on three U.S. Army bases in Hawai'i. Chapter III is the compilation of >32,000 home radon tests to create a 2018 Environmental Protection Agency (EPA) Indoor Radon Map of Texas. Each chapter has an abstract, introduction, analytical methods, results, discussion, conclusions, and references sections.

TABLE OF CONTENTS

CHAPTER I

FOURIER TRANSFORM MASS SPECTROMETRY: THE TRANSFORMATION OF MODERN ENVIRONMENTAL ANALYSES

(as published in International Journal of Molecular Sciences)

DOI: 10.3390/ijms17010104

ABSTRACT

Unknown compounds in environmental samples are difficult to identify using standard mass spectrometric methods. Fourier transform mass spectrometry (FTMS) has revolutionized how environmental analyses are performed. With its unsurpassed mass accuracy, high resolution and sensitivity, researchers now have a tool for difficult and complex environmental analyses. Two features of FTMS are responsible for changing the face of how complex analyses are accomplished. First is the ability to quickly and with high mass accuracy determine the presence of unknown chemical residues in samples. For years, the field has been limited by mass spectrometric methods that were based on knowing what compounds of interest were. Secondly, by utilizing the high-resolution capabilities coupled with the low detection limits of FTMS, analysts also could dilute the sample sufficiently to minimize the ionization changes from varied matrices.

INTRODUCTION

Toxic environmental chemical sources continue to be a problematic global health concern. There are multiple sources of pollutants which include agricultural, industrial, as well as other point sources such as mining, foundries and smelters, along with other metal-based industrial operations [1]. Excessive levels of pesticides in agricultural products and in herbal medicines are

also a concern with the public involved in healthcare [2]. Wastewater sludge that contains acidic contaminants is a growing area of concern as well [3]. These complex solid-liquid phase matrices require advanced high- performance

methods to monitor ultra-trace (part per trillion) levels of target compounds. Some of these have been detected even after the final purification stage in drinking water [4]. The presence of un-metabolized pharmaceuticals discharged into wastewater also is unavoidable with the current treatment processes in place [5]. Metal-based nanoparticles, which are an emerging pollutant stream, have been determined in the environment by inductively coupled plasma-mass spectrometry, for example [6]. The threat posed by nanoparticle pollution has become a difficult 21st century analytical problem. Diesel-burning engines are known to emit nanoparticles and these have been analyzed by thermal desorption particle beam mass spectrometry [7].

Fundamentally, environmental analyses consist of obtaining a representative sample, extracting the compound(s) of interest, performing appropriate sample clean-up, and deriving the concentration of the extract and determination of the compound identity and/or quantity. The United States Environmental Protection Agency (EPA) has collected resources including many environmental chemistry methods (ECMs) [8]. Environmental sample analyses typically have interference effects that result in poor quantitative data. Mass spectrometry requires that ions be produced in the gas phase. This may lead to sample preparation requiring extraction of the analyte from the matrix material or using matrix-matched calibration to compensate for matrix interferents. The preparation step results in diluting the analyte and thereby reducing the chances of recovering all trace chemical compound(s) of interest [9, 10]. Another issue with sample preparation is that matrix extraction may change the analyte's ionization efficiency, directly impacting detection limits [11]. The change may result in signal suppression or

enhancement. Differences in ionization may also occur due to the presence of solvent or matrix interference [9, 12]. Cost-effectiveness of sample analysis is a significant issue for environmental applications of mass spectrometry. Due to the complexity of many environmental samples, time-consuming and labor-intensive preparation steps are required to extract the compound of primary interest. This limited early investigations to targeted inquiries of study material [13].

Analytical ECMs have followed the improvements in mass spectrometers over the last decades. Initially, determinations were made with gas chromatography (GC) or liquid chromatography (LC) with specific detectors. These diverse detectors were rapidly replaced when mass spectrometry (MS) was mated to chromatographic separations in the hyphenated techniques of gas chromatography-mass spectrometry (GC-MS) and liquid chromatography-mass spectrometry (LC-MS). While GC-MS is still the workhorse for many environmental analyses, it is limited to compounds that can be volatilized without decomposition and are below 500 Da. It was recently noted that only organochlorine pesticides had better performance on GC-MS with all other classes of pesticides having wider scope and better sensitivity with LC-MS [14]. LC-MS has become the method of choice for many environmental applications.

Even though LC-MS has become a standard technique in many bio-related applications, it is recognized that a GC with 30 m of fused silica column provides much higher chromatographic resolution for small molecules. Various MS methods were employed in an attempt to make up for the lack of separating power of the shorter liquid chromatography columns. Chief among these methods was the use of tandem mass spectrometry (MS/MS or MS^2). Early ion traps were quickly adapted to perform MS/MS [15]. These MS/MS methods could now be used to determine a compound in a complex matrix by isolating the target ion of a compound followed by MS/MS to generate product ions confirming the identity of the target analyte. By interfacing

chromatography with MS/MS, specificities and sensitivities achieved were equivalent to radioimmunoassay and GC-MS [16]. This initiated a shift in research studies from target-oriented analyses to full scan mass spectrometry that has the capability to produce a complete mass spectrum of target molecules as well as determine molecules in unknown mixtures [17, 18]. This was initially seen as the answer to analyzing complex environmental samples. However, it has been reported that these low-resolution mass spectrometers were challenged when analyzing complex samples because of their low mass accuracy. For instance, in the determination of perfluorooctane sulfonate, an endogenous compound (cholate) has the same nominal mass for the precursor ion and product ions [19]. In these cases, an investigator can either perform better chromatography to separate the compound of interest from interferents or employ a mass spectrometer with a mass accuracy in the low ppm range. This MS approach is not always the answer, but has been investigated [20].

A MS review whose focus is on environmental applications is done biennially in Analytical Chemistry [21]. The current perspective is focused on high resolution Fourier transform mass spectrometry (FTMS) instrumentation that has accurate mass capabilities below 10 ppm. The high cost limits the availability of the Fourier transform ion cyclotron resonance (FT-ICR) MS instrumentation to many applications. The Orbitrap technology, on the other hand, has been increasing in popularity because of its lower cost and lack of cryogens, and the vast majority of current work has been performed using the Orbitrap platform for the analysis of demanding environmental applications. Therefore, this perspective will mainly focus on the Orbitrap.

FOURIER TRANSFORM ION CYCLOTRON RESONANCE (FT-ICR)

Fourier transform ion cyclotron resonance (FT-ICR) mass spectrometers are the gold standard because of their high resolution and their high accurate mass capability [22]. These ultra-high-resolution instruments enable the separation of isobaric species using their high accurate mass capabilities. This can be seen in Figure 1.1 which illustrates the low abundance ^{13}C ($^{13}CC_7H_{10}N_4O_2$) and ^{15}N ($C_8H_{10}N_3{}^{15}NO_2$) isotopes resolved for caffeine ($C_8H_{10}N_4O_2$).

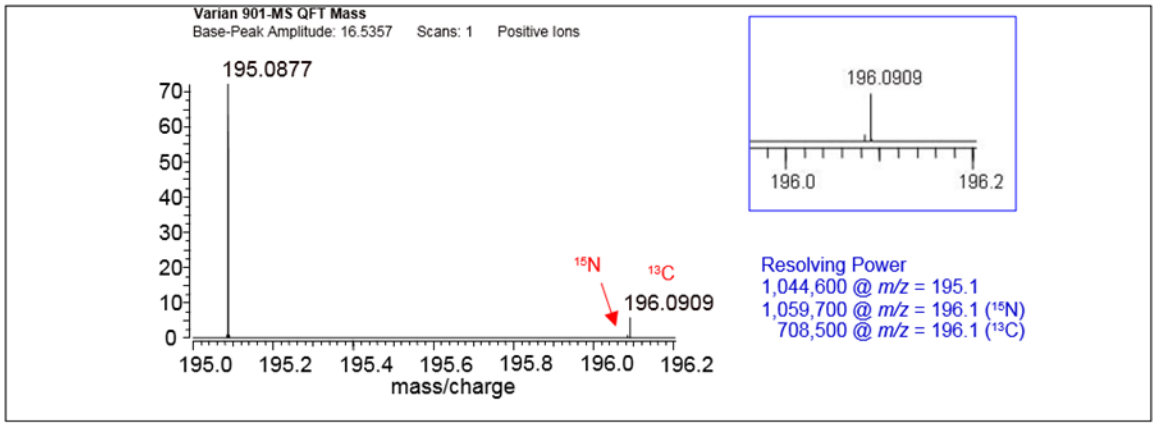

Figure 1.1. A high-resolution spectrum of caffeine analyzed with a Varian 901-MS-QFT (Mass Spectrometry-Quadrupole-Fourier Transform) mass spectrometer. The instrument was equipped with an electrospray ionization source (ZSpray) and a 9.4 T superconducting magnet.

FT-ICRs are very expensive instruments that require liquid helium-cooled superconducting magnets in order to operate. The high cost has kept these instruments only in advanced research laboratories and some academic settings. While it is clear that the mass resolution and the mass accuracy of these instruments is unsurpassed, the Orbitrap provides a more accessible and affordable avenue to high resolution and high mass accuracy. The usefulness of an Orbitrap

has been clearly stated by Makarov *et al.* [23]: “These levels of resolving power [of the Orbitrap] are still far below, and will remain below record values obtained in FT-ICR, but it is more than adequate even for most demanding complex mixtures such as petroleum or humic acids”.

ORBITRAP

The Orbitrap technology is a more widely available technology for high resolution MS (HRMS) with a high accuracy mass. Figure 1.2 shows two Orbitrap analyzers with both European and American coins as a reference for size. The smaller device is the newer ultra-high resolution Orbitrap analyzer.

Figure 1.2. Two Orbitrap analyzers with both a 1-Euro coin and an American nickel as a reference for size [24]. The smaller device is the newer ultra-high resolution Orbitrap analyzer.

The challenge in MS performance is measuring the *m*/*z* of a composition of ions across a wide molecular range. One option is to perform targeted analysis of a specific chemical, which is commonly done by using LC-MS/MS on triple-quadrupole mass spectrometers [25] Another approach is to implement untargeted analyses [26]. This “shotgun” method is an advanced development in MS to identify and quantify all the compounds in a sample simultaneously.

Orbitrap-based instruments with their higher sensitivity than more common quadrupole instruments can perform analysis on samples at greater dilutions to minimize the background interference. This mass spectrometer can be utilized for complex endogenous, exogenous or xenometabolite matrix samples [27-30]. For compounds mimicking environmentally relevant analytes, Figure 1.3 demonstrates the mass measurement accuracy and high resolutions attainable by these analyzers.

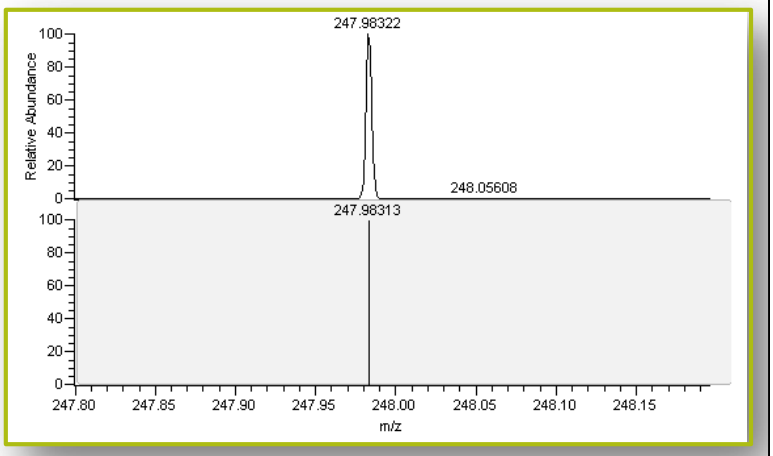

Rank	Formula	Δ ppm
1	$C_{12}H_9OBr$	4
2	$C_7H_5O_6N_2Cl$	6
3	$C_3H_2N_{10}Cl_2$	−1.3
4	$C_4H_8O_5N_3Cl_2$	−1.3
5	$C_9H_{12}NBrCl$	−1.6
6	$C_{10}H_2O_7N$	2.6
7	$C_2H_6O_4N_6Cl_2$	4.1
8	$C_8HO_2N_6Cl$	−4.8
9	$C_{10}H_7N_3Br$	5.8

Figure 1.3. The importance of high mass accuracy: The high mass accuracy allows researchers to limit the number of possible molecular formulae significantly based on the accurate mass measurement. Here the correct formula, $C_{12}H_9OBr$ (1-bromo-4-phenoxy-benzene), is the highest ranked formula based on lowest mass error. While other molecular formulas are possible, they can be excluded when combined with knowledge of the target ion. Used with permission from Thermo Scientific; Waltham, MA, USA.

The Orbitrap is considered by many users as a robust analyzer that provides quantitative data on both clinical and environmental molecular biomarkers [31]. The Orbitrap has been

typically mated to LC [32], and coupling with GC was introduced recently [33]. The ionization options for LC-MS include electrospray ionization (ESI), nanospray (nESI), atmospheric pressure chemical ionization (APCI) and atmospheric pressure photoionization (APPI), while for the GC-MS instrument the available ionization is either electron impact (EI) or chemical ionization (CI).

Descriptions of the Orbitrap and its operational theory are fully covered in prior work [34]. Once the ions are transferred into the Orbitrap analyzer, the ions are trapped in an electrostatic field created by both the spindle and outer electrodes [35, 36]. The trapped ions move radially and oscillate along a central spindle (Orbitrap) electrode. The mass accuracy of the Orbitrap instrument is 2–5 ppm [37]. In the current models, <1 ppm mass accuracy is obtained with internal calibration while for external calibration the mass accuracy is specified as <3 ppm. The mass resolution of the classic Orbitrap analyzer can be up to 150,000 while the new ultra-high field Orbitrap analyzers have resolving power of more than 600,000 [23].

The ion traps of hybrid instruments are also capable of performing multiple MS steps, which aids in elucidating important structural information [38]. A search of case studies utilizing this technology reveals that there are applications for emerging environmental contaminants [39].

SELECTED ENVIRONMENTAL APPLICATIONS OF THE ORBITRAP

A single-stage Orbitrap-MS was used to identify and quantify non-targeted analytes in a U.S. Food and Drug Administration (FDA) study testing dog food. These results were compared to a targeted method based on a triple-quadrupole LC-MS/MS [40]. The biomonitoring of pesticides in urine [41] and the confirmatory analysis for growth-promoting agents in meat production [42] has accurately been determined using Orbitrap high resolution MS analyzers.

The identification of fullerenes in wastewater matrices was determined and quantified using an Orbitrap [43, 44]. This technology enabled fewer sampling repetitions which allowed for an increased sample throughput and less wasted sample [42]. Optimization of matrix effects from sewage water (influent and effluent) improved the detection of metabolites and showed satisfactory recovery and precision for most known compounds [28, 45, 46]. Additional examples of successful screening using an Orbitrap include the determination of pesticide levels in soils and food [47] and various plant and fungal metabolites discovered in animal feed [48].

The elucidation of structural fragments without any pre-treatment was reported for metabolomic analysis of green and black tea extracts using an LTQ Orbitrap XL (a hybrid linear ion trap Orbitrap mass spectrometer) [49], and for direct analysis of red wine using ultra-fast chromatography and high resolution MS [50]. Rapid screening of textile samples for 19 human health and environmental toxins using a LTQ Orbitrap achieved a limit of quantitation (LOQ) lower than the adopted European Union regulations [51].

The level of pharmaceutical metabolites and parent compounds in surface waters has increased in both treated waste water and drinking water. This problem was addressed when a LTQ Orbitrap was used to provide better data for these complex matrices [52]. Mycotoxins and pesticide residues

in agricultural products have become a serious human health concern. A high-throughput method was developed using an Orbitrap for high resolution MS after a single-stage extraction in spice analysis [53].

The emerging use of nanotechnology to enhance the properties of a variety of products has potential negative impacts to health and safety. In order to adequately evaluate the environmental risks requires further study of these nanomaterials using advanced mass

spectrometry–based analytical techniques [54]. Screening surface water samples for related transformation products of nanomaterials has directly benefitted from the LTQ Orbitrap. The LC-LTQ-Orbitrap MS analysis was developed in part to provide a better screening technology for surface water samples that might contain these transformation products of nanomaterials [55].

Screen methods for emerging contaminants (new target compounds) in wastewater effluent, surface and ground water, along with finished drinking water can be reliably developed using the LTQ Orbitrap [39]. These newly developed work flows have demonstrated high-throughput sample processing using the most advanced LC-Orbitrap platform. A recent study indicated a rapid separation of targeted analytes within 14 min [56]. With the improved reliability for the detection of these emerging contaminants, the manufacturing companies and waste water treatment facilities will face stronger regulatory pressure for removal of these contaminants in the manufacturing processes. This is especially important for the hydrophilic compounds that are inherently more difficult to remove from complex mixtures [57].

CONCLUSIONS

The Orbitrap mass spectrometer with its high resolution and high mass accuracy capabilities has demonstrated that it is a powerful analytical tool in the investigation of the fate of environmental contaminants in complex matrices and mixtures [58]. The databases for identifying environmental contaminants continue to expand [41]. In addition, newly developed data analysis software and database search tools (e.g., spectral library searching, literature data) for the identification of emerging environmental contaminants in the aquatic environment aid in advancing the utility of this analytical platform [59]. The high resolution (R > 100,000) and

accurate mass (mass error < 2 ppm) capabilities of the Orbitrap provide many new opportunities for applications in environmental research [60].

No one mass spectrometric technique is ideal for all applications in research in clinical and environmental settings. This technology is rapidly developing, and the future benefits are based upon the application, cost and performance desired. The FTMS technology has proven to be beneficial for many difficult analytical environmental questions. There are many different models of FTMS now available. While the FT-ICR is and will remain the ultimate standard for highest resolution MS and mass accuracy, the Orbitrap has proven to be more affordable and is highly applicable to answer many of these complex analytical/environmental questions. The ability to "dilute and shoot" may be one of the most important values of this FTMS technology. By diluting interfering substances, ionization is much less affected by enhancement or suppression. In this context, the U.S. Food and Drug Administration's (FDA) Guidance for Industry: Bioanalytical Method Validation [61] recommends incurred sample reanalysis (ISR) in order to assess reproducibility, which also should be considered in environmental analyses. The use of FTMS is unparalleled in that role. High mass accuracy can eliminate questions of false positives that have been shown to exist with low resolution mass spectrometric methods [62]. In critical situations, FTMS can provide the necessary unambiguous answers through a combination of high resolution and high mass accuracy that analysts seek to provide.

ACKNOWLEDGMENTS

Support for this project was provided by the Department of Environmental Toxicology, Texas Tech University, Lubbock, TX 79409, USA.

REFERENCES

1. Tchounwou, P.B.; Yedjou, C.G.; Patlolla, A.K.; Sutton, D.J. Heavy metals toxicity and the environment. *EXS* **2014**, *101*, 133–164.
2. Chan, K. Some aspects of toxic contaminants in herbal medicines. *Chemosphere* **2003**, *52*, 1361–1371.
3. Cahill, M.G.; Dineen, B.A.; Stack, M.A.; James, K.J. A critical evaluation of liquid chromatography with hybrid linear ion trap—Orbitrap mass spectrometry for the determination of acidic contaminants in wastewater effluents. *J. Chromatogr. A* **2012**, *1270*, 88–95.
4. De Sena, R.F.; Tambosi, J.L.; Moreira, F.P.M.; José, H.J.; Gebhardt, W.; Schröder, H.F. Evaluation of sample processing methods for the polar contaminant analysis of sewage sludge using liquid chromatography-mass spectrometry. *Quim. Nova* **2010**, *33*, 1194–1198.
5. Hirsch, R.; Ternes, T.; Haberer, K.; Kratz, K.-L. Occurrence of antibiotics in the aquatic environment.
   Sci. Total Environ. **1999**, *225*, 109–118.
6. Huang, C.; Hu, B. Silica-coated magnetic nanoparticles modified with γ-mercaptopropyltrimethoxysilane for fast and selective solid phase extraction of trace amounts of Cd, Cu, Hg, and Pb in environmental and biological samples prior to their determination by inductively coupled plasma mass spectrometry. *Spectrochim. Acta Part B* **2008**, *63*, 437–444.
7. Tobias, H.J.; Beving, D.E.; Ziemann, P.J.; Sakurai, H.; Zuk, M.; McMurry, P.H.; Zarling, D.; Waytulonis, R.; Kittelson, D.B. Chemical analysis of diesel engine nanoparticles using a nano-DMA/thermal desorption particle beam mass spectrometer. *Environ. Sci. Technol.* **2001**, *35*, 2233–2243.
8. Environmental Chemistry Methods (ECM). Available online: http://www2.epa.gov/pesticide-analytical-methods/environmental-chemistry-methods-ecm (accessed on 12 January 2016).
9. Mitigating Matrix Effects: Examination of Dilution, QuEChERS, and Calibration Strategies for LC-MS/MS Analysis of Pesticide Residues in Diverse Food Types. Available online: http://www.restek.com/Technical-Resources/Technical-Library/Foods-Flavors-Fragrances/fff_FFAN1796A-UNV (accessed on 12 January 2016).
10. Garg, N.; Kapono, C.A.; Lim, Y.W.; Koyama, N.; Vermeij, M.J.A.; Conrad, D.; Rohwer, F.; Dorrestein, P.C. Mass spectral similarity for untargeted metabolomics data analysis of complex mixtures. *Int. J. Mass Spectrom.* **2015**, *377*, 719–727.
11. Zielinski, T.; Pazdro, K.; Dragan-Górska, A.; Weydmann, A. *Insights on Environmental Changes*; Springer: New York, NY, USA, 2014.
12. McEwen, C.N.; Larsen, B.S. Fifty years of desorption ionization of nonvolatile compounds. *Int. J. Mass Spectrom.* **2015**, *377*, 515–531.
13. Romero-Gonzalez, R. Food safety: How analytical chemists ensure it. *Anal. Methods* **2015**, *7*, 7193–7201.
14. Alder, L.; Greulich, K.; Kempe, G.; Vieth, B. Residue analysis of 500 high priority pesticides: Better by GC–MS or LC–MS/MS? *Mass Spectrom. Rev.* **2006**, *25*, 838–865.
15. Louris, J.N.; Cooks, R.G.; Syka, J.E.; Kelley, P.E.; Stafford, G.C., Jr.; Todd, J.F. Instrumentation, applications, and energy deposition in quadrupole ion-trap tandem mass spectrometry. *Anal. Chem.* **1987**, *59*, 1677–1685.

16. Yates, J.R.; Cociorva, D.; Liao, L.; Zabrouskov, V. Performance of a linear ion trap-Orbitrap hybrid for peptide analysis. *Anal. Chem.* **2006**, *78*, 493–500.
17. Van Meulebroek, L.; Vanden Bussche, J.; Steppe, K.; Vanhaecke, L. High-resolution Orbitrap mass spectrometry for the analysis of carotenoids in tomato fruit: Validation and comparative evaluation towards UV-VIS and tandem mass spectrometry. *Anal. Bioanal. Chem.* **2014**, *406*, 2613–2626.
18. Sokol, E.; Almeida, R.; Hannibal-Bach, H.K.; Kotowska, D.; Vogt, J.; Baumgart, J.; Kristiansen, K.; Nitsch, R.; Knudsen, J.; Ejsing, C.S. Profiling of lipid species by normal-phase liquid chromatography, nanoelectrospray ionization, and ion trap-Orbitrap mass spectrometry. *Anal. Biochem.* **2013**, *443*, 88–96.
19. Chan, E.; Sandhu, M.; Benskin, J.P.; Ralitsch, M.; Thibault, N.; Birkholz, D.; Martin, J.W. Endogenous high-performance liquid chromatography/tandem mass spectrometry interferences and the case of perfluorohexane sulfonate (PFHxS) in human serum; are we overestimating exposure? *Rapid Commun. Mass Spectrom.* **2009**, *23*, 1405–1410.
20. Croley, T.; White, K.; Callahan, J.; Musser, S. The chromatographic role in high resolution mass spectrometry for non-targeted analysis. *J. Am. Soc. Mass Spectrom.* **2012**, *23*, 1569–1578.
21. Richardson, S.D. Environmental mass spectrometry: Emerging contaminants and current issues. *Anal. Chem.* **2011**, *84*, 747–778.
22. Marshall, A.G.; Hendrickson, C.L.; Jackson, G.S. Fourier transform ion cyclotron resonance mass spectrometry: A primer. *Mass Spectrom. Rev.* **1998**, *17*, 1–35.
23. Makarov, A.; Denisov, E.; Lange, O. Performance evaluation of a high-field Orbitrap mass analyzer. *J. Am. Soc. Mass Spectrom.* **2009**, *20*, 1391–1396.
24. Orbitrap Mass Analyzers. Available online: http://www.thermoscientific.com/en/products/orbitrap-lc-ms.html (accessed on 12 January 2016).
25. Henion, J.; Brewer, E.; Rule, G. Sample preparation for LC/MS/MS: Knowing the basic requirements and the big picture of an LC/MS system can ensure success in most instances. *Anal. Chem.* **1998**, *70*, 650A–656A.
26. Turnipseed, S.B.; Lohne, J.J.; Boison, J.O. Review: Application of high resolution mass spectrometry to monitor veterinary drug residues in aquacultured products. *J. AOAC Int.* **2015**, *98*, 550–558.
27. Shi, Y.; Chang, J.S.; Esposito, C.L.; Lafontaine, C.; Berube, M.J.; Fink, J.A.; Espourteille, F.A. Rapid screening for pesticides using automated online sample preparation with a high-resolution benchtop Orbitrap mass spectrometer. *Food Addit. Contam. Part. A* **2011**, *28*, 1383–1392.
28. Ruan, Q.; Peterman, S.; Szewc, M.A.; Ma, L.; Cui, D.; Humphreys, W.G.; Zhu, M. An integrated method for metabolite detection and identification using a linear ion trap/Orbitrap mass spectrometer and multiple data processing techniques: Application to indinavir metabolite detection. *J. Mass Spectrom.* **2008**, *43*, 251–261.
29. Rudashevskaya, E.L.; Breitwieser, F.P.; Huber, M.L.; Colinge, J.; Muller, A.C.; Bennett, K.L. Multiple and sequential data acquisition method: An improved method for fragmentation and detection of cross-linked peptides on a hybrid linear trap quadrupole Orbitrap Velos mass spectrometer. *Anal. Chem.* **2013**, *85*, 1454–1461.

30. Schrader, W.; Xuan, Y.; Gaspar, A. Studying ultra-complex crude oil mixtures by using high-field asymmetric waveform ion mobility spectrometry (FAIMS) coupled to an electrospray ionisation-LTQ-Orbitrap mass spectrometer. *Eur. J. Mass Spectrom.* **2014**, *20*, 43–49.
31. Ahlf, D.R.; Compton, P.D.; Tran, J.C.; Early, B.P.; Thomas, P.M.; Kelleher, N.L. Evaluation of the compact high-field Orbitrap for top-down proteomics of human cells. *J. Proteome Res.* **2012**, *11*, 4308–4314.
32. Makarov, A.; Denisov, E.; Kholomeev, A.; Balschun, W.; Lange, O.; Strupat, K.; Horning, S. Performance evaluation of a hybrid linear ion trap/Orbitrap mass spectrometer. *Anal. Chem.* **2006**, *78*, 2113–2120.
33. Peterson, A.C.; Balloon, A.J.; Westphall, M.S.; Coon, J.J. Development of a GC/quadrupole-Orbitrap Mass spectrometer, part II: New approaches for discovery metabolomics. *Anal. Chem.* **2014**, *86*, 10044–10051.
34. Zubarev, R.A.; Makarov, A. Orbitrap mass spectrometry. *Anal. Chem.* **2013**, *85*, 5288–5296.
35. Michalski, A.; Damoc, E.; Hauschild, J.P.; Lange, O.; Wieghaus, A.; Makarov, A.; Nagaraj, N.; Cox, J.; Mann, M.; Horning, S. Mass spectrometry-based proteomics using Q exactive, a high-performance benchtop quadrupole Orbitrap mass spectrometer. *Mol. Cell. Proteom.* **2011**, *10*, doi:10.1074/mcp.M111.011015.
36. Scigelova, M.; Makarov, A. Orbitrap mass analyzer—Overview and applications in proteomics. *Proteomics* **2006**, *6*,16–21.
37. *Scientific C: LC/GC's Chromacademy*; Crawford Scientific: Duluth, MN, USA, 2014.
38. Bijttebier, S.K.; D'Hondt, E.; Hermans, N.; Apers, S.; Voorspoels, S. Unravelling Ionization and Fragmentation pathways of carotenoids using Orbitrap technology: A first step Towards Identification of Unknowns. *J. Mass Spectrom.* **2013**, *48*, 740–754.
39. Hogenboom, A.C.; van Leerdam, J.A.; de Voogt, P. Accurate mass screening and identification of emerging contaminants in environmental samples by liquid chromatography–hybrid linear ion trap Orbitrap mass spectrometry. *J. Chromatogr. A* **2009**, *1216*, 510–519.
40. Lohne, J.J.; Turnipseed, S.B.; Andersen, W.C.; Storey, J.; Madson, M.R. Application of single stage Orbitrap mass spectrometry and differential analysis software to non-targeted analysis of contaminants in dog food: Detection, identification, and quantification of glycoalkaloids. *J. Agric. Food Chem.* **2015**, *63*, 4790–4798.
41. Roca, M.; Leon, N.; Pastor, A.; Yusa, V. Comprehensive analytical strategy for biomonitoring of pesticides in urine by liquid chromatography-Orbitrap high resolution masss pectrometry. *J. Chromatogr. A* **2014**, *1374*, 66–76.
42. Usansky, J. Integrating Laboratory Information Management Systems with LC-MS/MS Systems for Incurred Sample Reanalysis. In *White Paper*; Thermo Fisher Scientific: Waltham, MA, USA, 2011.
43. Huang, F.; Ge, L.; Zhang, B.; Wang, Y.; Tian, H.; Zhao, L.; He, Y.; Zhang, X. A fullerene colloidal suspension stimulates the growth and denitrification ability of wastewater treatment sludge-derived bacteria. *Chemosphere* **2014**, *108*, 411–417.
44. Herrero, P.; Bäuerlein, P.S.; Emke, E.; Marcé, R.M.; Voogt, P. Size and concentration determination of (functionalised) fullerenes in surface and sewage water matrices using field flow fractionation coupled to an online accurate mass spectrometer: Method development and validation. *Anal. Chim. Acta* **2015**, *871*, 77–84.

45. Bijlsma, L.; Emke, E.; Hernandez, F.; de Voogt, P. Performance of the linear ion trap Orbitrap mass analyzer for qualitative and quantitative analysis of drugs of abuse and relevant metabolites in sewage water. *Anal. Chim. Acta* **2013**, *768*, 102–110.
46. Barry, J.A.; Groseclose, M.R.; Robichaud, G.; Castellino, S.; Muddiman, D.C. Assessing drug and metabolite detection in liver tissue by UV-MALDI and IR-MALDESI mass spectrometry imaging coupled to FT-ICR MS. *Int. J. Mass Spectrom.* **2015**, *377*, 448–455.
47. Alder, L.; Steinborn, A.; Bergelt, S. Suitability of an Orbitrap mass spectrometer for the screening of pesticide residues in extracts of fruits and vegetables. *J. AOAC Int.* **2011**, *94*, 1661–1673.
48. Ates, E.; Godula, M.; Stroka, J.; Senyuva, H. Screening of plant and fungal metabolites in wheat, maize and animal feed using automated on-line clean-up coupled to high resolution mass spectrometry. *Food Chem.* **2014**, *142*, 276–284.
49. Wilson, D.L.; Yang, C. Metabolomic analysis of green and black tea extracts using an LTQ Orbitrap XL hybrid linear ion trap mass spectrometer. *Thermo Scie.* **2008**, Application note 420. Avaliable online: https://www.thermofisher.co.nz/Uploads/file/Scientific/Applications/Scientific-Instruments-Automation/Metabolomic-Analysis-of-Green-and-Black-Tea-Extracts-Using-an-LTQ-Orbitrap-XL-Hybrid-Linear-Ion-Trap-Mass-Spectrometer.PDF (accessed on 12 January 2016).
50. Damoc, E.; Pehal, F.; Hornshaw, M. Direct analysis of red wine using ultra-fast chromatography and high resolution mass spectrometry. *J. Sep. Sci.* **2009**, *32*, 3854.
51. Zhang, L.; Luo, X.; Niu, Z.; Ye, X.; Tang, Z.; Yao, P. Rapid screening and identification of multi-class substances of very high concern in textiles using liquid chromatography-hybrid linear ion trap Orbitrap mass spectrometry. *J. Chromatogr. A* **2015**, *1386*, 22–30.
52. Favier, M.; Dewil, R.; van Eyck, K.; van Schepdael, A.; Cabooter, D. High-resolution MS and MS^n investigation of ozone oxidation products from phenazone-type pharmaceuticals and metabolites. *Chemosphere* **2015**, *136*, 32–41.
53. Reinholds, I.; Pugajeva, I.; Bartkevics, V. A reliable screening of mycotoxins and pesticide residues in paprika using ultra-high performance liquid chromatography coupled to high resolution Orbitrap mass spectrometry. *Food Control.* **2016**, *60*, 683–689.
54. Zhang, B.; Misak, H.; Dhanasekaran, P.S.; Kalla, D.; Asmatulu, R. Environmental Impacts of Nanotechnology and Its Products. In Proceedings of the 2011 Midwest Section Conference of the American Society for Engineering Education, Russellville, Arkansas, 29 September 2011.
55. Van Wezel, A.P.; Morinière, V.; Emke, E.; ter Laak, T. Hogenboom, A.C. Quantifying summed fullerene nC_{60} and related transformation products in water using LC LTQ Orbitrap MS and application to environmental samples. *Environ. Int.* **2011**, *37*, 1063–1067.
56. Zacs, D.; Bartkevics, V. Analytical capabilities of high performance liquid chromatography–Atmospheric pressure photoionization-Orbitrap mass spectrometry (HPLC-APPI-Orbitrap-MS) for the trace determination of novel and emerging flame retardants in fish. *Anal. Chim. Acta* **2015**, *898*, 60–72.
57. Radjenovic, J.; Petrovic, M.; Barceló, D. Analysis of pharmaceuticals in wastewater and removal using a membrane bioreactor. *Anal. Bioanal. Chem.* **2007**, *387*, 1365–1377.
58. Barceló, D.; Petrovic, M. Challenges and achievements of LC-MS in environmental analysis: 25 years on. *TrAC Trends Anal. Chem.* **2007**, *26*, 2–11.

59. Mol, H.J.; Zomer, P.; de Koning, M. Qualitative aspects and validation of a screening method for pesticides in vegetables and fruits based on liquid chromatography coupled to full scan high resolution (Orbitrap) mass spectrometry. *Anal. Bioanal. Chem.* **2012**, *403*, 2891–2908.
60. Makarov, A.; Scigelova, M. Coupling liquid chromatography to Orbitrap mass spectrometry. *J. Chromatogr. A* **2010**, *1217*, 3938–3945.
61. Food and Drug Administration. FDA guidance for industry: Bioanalytical method validation. Rockville, MD: US Department of Health and Human Services. *Food Drug Adm. Center Drug Eval. Res.* **2001**, *1*, 124–129.
62. Krauss, M.; Hollender, J. Analysis of nitrosamines in wastewater: Exploring the trace level quantification capabilities of a hybrid linear ion trap/Orbitrap mass spectrometer. *Anal. Chem.* **2008**, *80*, 834–842.

CHAPTER II

INVESTIGATION OF DEPLETED URANIUM IN HAWAI'I SOIL SAMPLES

ABSTRACT

In Hawai'i the use of depleted uranium (DU) ordnance on Schofield Barracks Firing Range was disclosed by the U.S. Army in 2005 after corroded projectile remnants were discovered during field inspection of firing ranges. The metal was used during the 1960s in a portable nuclear assembly known as the Davy Crockett weapon system. This classified military arsenal was initially developed to deploy small nuclear warheads for tactical use on overseas battlefield objectives during the Cold War. Depleted uranium was used as a substitute in the practice projectiles (i.e., M101) because of the near identical density to the radioactive materials intended for use during war. Depleted uranium would mimic the trajectory of the larger caliber ordnance designed for combat. Since the original field findings in Hawai'i, the U.S. Army surveyed additional firing ranges on other Hawaiian Island military bases that may have used the depleted uranium and declared any discovered depleted uranium in the environment was contained. The focus of this study was to use Inductively Coupled Plasma - Mass Spectrometer (ICP-MS) to determine the isotope ratio concentration of uranium ($^{235}U/^{238}U$) in surface soils off-site from the military's contained radiation control areas, as well as off-base areas near communities. Uranium isotope ratios, using ICP-MS counts-per-second (CPS), that were lower in values from natural background levels (0.007257) would indicate infiltration from human activities with high levels of ^{238}U. Off-base findings would be a consequence of migration away from the restricted shooting range areas, becoming a potential impact to the environment and

human health. This study consisted of 13 grab samples in areas on- and off-military installations that yielded uranium isotope ratios with three point-sources that have uranium isotope ratios below the idealized value. These three point-sources are certain candidates for expanded analysis.

INTRODUCTION

Many actinides, which include uranium and its isotopes, are radioactive and release ionizing energy upon radioactive decay.[1] For this reason, depleted uranium used in conventional military ordnance in combat or training has potential risks to humans and the environment on both short- and long-term time-scales. In addition, after firing these contaminants of concern become heterogeneously distributed in soil and will ultimately redistribute away from the initial point of deposition due to wind and rain events.[2]

Depending on the duration and dose of exposure to depleted uranium residues, this metal is considered the causative agent of an increased array of human pathologies that have occurred near combat areas.[3-5] Early toxicology studies of uranium using chronic low-dose, or subacute exposure attributed no definitive set of toxicological symptoms to human health, which was the basis for its use in combat and training by the U.S. military.[6, 7] Despite the testament of uranium's low health risk, civilian communities living in active combat areas have been affected by an array of physiological changes that are claimed to be linked to depleted uranium's presence.[8] Some Hawaiian residents on the Big Island believe that areas with increased health problems originated from inhalation of depleted uranium used in the 1960s field training. Inadequate abatement only continues to pollute the air through soil dust carried downwind from its origin.[9] Our surface soil analysis in this study used ICP-MS, a sensitive method to analyze

environmental uranium isotope ratios, to ascertain migration away from three restricted radiological military zones on two Hawaiian Islands.

NATURAL URANIUM

Natural uranium (NU) is found in 249 mineral ore species[10] and occurs naturally in soil worldwide. Uranium has two naturally occurring parent isotopes and all isotopes are radioactive.[11] An enrichment process of natural ore concentrates the uranium-235 (^{235}U), which leaves behind 99.8% of ^{238}U by mass.[12]-[13] The concentrated ^{235}U is enriched uranium (EU) for use in generating the high energy required to fuel thermal- and fast-neutron nuclear reactor operations and developing nuclear armaments. [14] The remaining by-product of the enrichment process is called depleted uranium (DU), which is 40% less radioactive compared to an equal quantity of natural ore.[15]). As defined by the Nuclear Regulatory Commission (NRC), depleted uranium has 0.2–0.3 % of ^{235}U while ^{238}U comprises the remaining 98.7–98.8 % of product.[16] This separation of ^{235}U relative to ^{238}U permits the application of sensitive analytical methods to measure $^{235}U/^{238}U$ ratios, which is significantly higher in depleted uranium products compared to the uranium ratio in the natural environment (Figure 1).[13, 17, 18] In nature, mass concentration of uranium varies widely, however, the percentage of uranium isotopes is considered invariant[19] without addition by an anthropogenic source. The isotope ratio is proportional to the mass difference between the two isotopes studied in the natural terrestrial system, per the 'normal mass dependence rule'.[20] This consideration has led to a widely used consensus value for the $^{235}U/^{238}U$ ratio of 0.007257 (uncertainty < 0.02% (2σ)) for current day naturally occurring ratio calculations, but slight geographical variations occur and are used as a geological chemical fingerprint for some sites.[19]

Over time, depleted uranium will mix with natural uranium in soil, which can relate any existing depleted uranium fraction (X, mg) according to the mathematical equation[21]: [Eqn. 1]

$$\frac{0.72 - 0.37X}{99.2745 + 0.3755X}$$

Depleted uranium, defined as 0.2% , is used in the discovery ratio estimates of $^{235}U/^{238}U$ in soil. Equation 1 is applied to determine the depleted uranium fraction in soil that may be mixed with natural uranium, which yields ratios tabulated in Table 2.1:

Table 2.1: Estimated $^{235}U/^{238}U$ ratio using Eqn 1; depleted uranium (DU) fraction 'X%' of total uranium in sample

$^{235}U/^{238}U$ ratio	%NU soil	%DU (^{235}U = 0.2%)
0.0072	100%	0%
0.00673	90%	10%
0.0062	80%	20%
0.00567	70%	30%
0.00515	60%	40%
0.00462	50%	50%
0.0041	40%	60%
0.00357	30%	70%
0.00305	20%	80%
0.00253	10%	90%
0.002	0%	100%

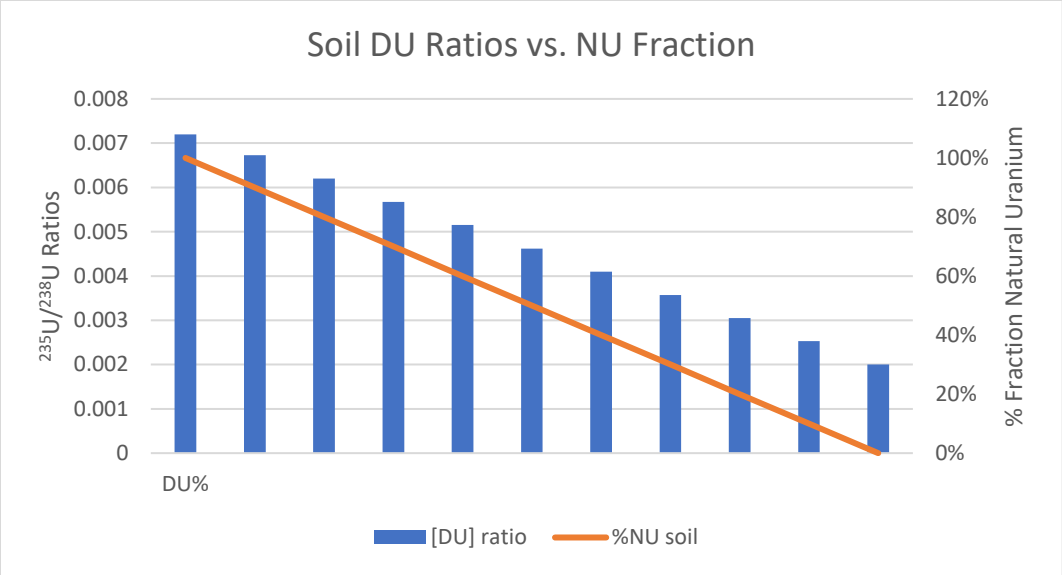

Figure 2.1: Graph of Table 1. Assuming an 'X' amount of depleted uranium with resultant $^{235}U/^{238}U$ ratio variations when mixed with natural uranium.

URANIUM'S HEALTH CONCERN

Uranium is regularly ingested primarily through dietary consumption of plant roots[22, 23], water intake, and air[24] yielding nearly 90 µg of uranium in our body.[25] Soluble uranium, considered five times more toxic than insoluble compounds[26] is absorbed in our digestive tract, 0.2% and 2% in food and water respectively, which then may enter our bloodstream to be filtered through the kidneys.[27] The intestinal tract does not easily absorb insoluble uranium, which results in lower dose intakes.[28] The Environmental Protection Agency (EPA) and the World Health Organization (WHO) have recommended a maximum contaminant level (MCL) and guideline level value (EPA and WHO, respectively) for uranium in publicly distributed drinking water and groundwater at 30 µg/L (parts per billion, ppb), which is based on the metal's chemical toxicity alone.[29, 30] The human dietary intake of uranium is

estimated to be in the range of 0.9 to 1.5 µg per day.[31] The daily "minimal risk" oral uptake exposure for humans is designated at 2 µg of uranium per kg body weight.[32]

The alpha particles emitted by uranium from decay, which are less penetrating than other forms of radiation, cause little harm if encountered outside the body.[33] However, when inhaled or ingested, its ionizing radiation has been shown to increase lung cancer and renal abnormality risks, respectively.[34, 35] This internal deposition is considered by governmental and international organizations to be the primary exposure route for exposed military and civilians in war-torn countries.[36] Because of the similar harmful biological outcomes from both of these effects, it is difficult to differentiate which physical property is responsible for any observed harmful outcome.[37]

THE VALUE OF DEPLETED URANIUM (DU)

DU's Propitious Physical Characteristics: Commercial Uses and Military Conventional Ordnance

Uranium's high density (68.4 % greater than lead), is suited for its use as counterbalance weights and ballasts on ships, airplanes, and forklifts. (Use in airplanes varies from 12 – 83 lbs. (5.4 – 37.6 kg) per unit using 21 – 31 units per tail assembly; nearly 692 – 1059 lbs. (314 – 480.4 kg) per Boeing aircraft produced 1968 - 1981).[38] Depleted uranium is also used commercially as radioactive shielding for workers in medical radiotherapy facilities[39] and medical imaging laboratories (e.g., X-ray and magnetic resonance imaging (MRI)). Depleted uranium material is combined with cement to construct lighter and smaller storage casks to hold and transport radioactive waste.[40] A novel use proposed for depleted uranium is the production of solar cells.[41]

The high density of depleted uranium also makes it useful to the military for reinforcing vehicle armor to survive conventional munition attacks. The density of uranium (18.8 g/cm^3) is comparable to tungsten (^{184}W, 19.6 g/cm^3), the metal that was historically used for ordnance production.[42] However, the costs and availability of depleted uranium are significantly less compared to tungsten production[43] particularly since a significant stockpile has been accumulated since the 1950s.[44] In addition, depleted uranium use is considered superior in target penetration because depleted uranium bullets will increase in tip sharpness as the bullet tip 'shreds' to a pointed-tip as it pierces through a 'hardened' (metal) object.[45] Additionally, the pyrophoric property of uranium more effectively eliminates a target without the need for the addition of explosives to obliterate the military target from further use or occupancy.[46]

Use of High-Velocity Penetrator Rounds: Depleted Uranium Aerosols from 'Hard' Target Explosions

Depleted uranium ordnance use during the Gulf War I (1990-1991), Kosovo War (1998-1999), Gulf War II (2003-2011), is estimated at 286 to 320 metric tons (286,000 kg)[47], 11 tons (~10,000 kg), and 75 tons (~68,000 kg), of depleted uranium respectively.[48] Each 30-mm penetrator round used consists of nearly 280 g of depleted uranium, while each 120 mm round used consists of 4.7 kg.[49] At impact the penetrators fragment generating aerosols composed of various uranium oxide mixtures (UO_2, UO_3 and U_3O_8).[27, 50] The destruction of a 'hard' target will generate a plume of <5 micron (μm)-sized particles.[51] The dispersion of these micro-particles may become a public health concern due to being both chemically toxic and radioactive.[37, 52] Inhalation of aerosol particles with diameters less than 10 μm pass the larynx and ciliated airways, allowing entry into the lower respiratory tract.[53]

Environmental soil surveys from Kosovo,[54-56] and the Bosnia/Herzegovina war zones[51, 57, 58] found that substantial depleted uranium contamination settled within meters of the point of armored-target impact, but levels above background were deposited up to 183 meters (m) away depending on the weapon caliber, the target-type impacted, and weather conditions.[4, 59-61] For this reason, communities within 50 m of an impact site are considered at the highest risk of inhalation exposure, even decades later due to remnant weathering and corrosion.[62, 63] The inhalation risk remains possible from any disturbance of small, inhalable, insoluble, weathered depleted uranium particles that remain in soils.[42, 64] Isotopic testing of these contaminated areas noted high $^{235}U/^{238}U$ ratios above background, with the lowest ratio concentration of 0.002147 (western Kosovo study area).[51, 54, 65]

CARCINOGENICITY OF DEPLETED URANIUM

The Environmental Protection Agency (EPA) has classified all radionuclides, which are unstable atoms that emit radiation, as a Group A carcinogen if inhaled or ingested.[66] This classification includes depleted uranium and its isotopes. Toxic health effects are related to the exposure dose, frequency, and duration of exposure and exposure route (oral, inhalation, dermal). Clinical symptoms, such as cancer or genetic effects, may not manifest for many years.[67] Exposure to high doses of uranium can be cytotoxic and clastogenic to lung tissue cell DNA.[68-71] The radiation, particles or rays that are released upon decay, has energy to ionize electrons from the body's water, protein, and DNA molecules when they interact.[72] The kidney is considered the target organ for uranium toxicity, and screening for exposure is performed using creatinine levels in urine (formulated to account for dilute urines).[35, 73, 74] Any elevated levels were transitory and values returned to normal after uranium removal.[75,

76] Abnormal medical outcomes, such as cancer or genetic effects, may not manifest for many years, if at all.[67] Despite these possibilities, no human morbidity or mortality findings from uranium exposure have been associated with oral or inhalation exposures to dust or fine particulates of uranium oxides, which are relatively insoluble and tend to be retained within the lung longer.[77-80]

DEPLETED URANIUM SOIL MIGRATION

It is crucial to understand the geologic, mineralogic, and chemical occurrences of metals in earth materials to effectively predict metal mobility in the environment. The mobility of uranium metal increases when it changes into an oxidized form. Uranium oxides may exist in both sparingly soluble, UO_2 [U(IV), +4 state, uranium dioxide], and insoluble, U_3O_8 [U(VI), +6 state, triuranium octoxide] forms.[25] Moreover, weathering on the surface of an un-oxidized metal (e.g., shrapnel) particle may react with the surrounding soil humic acids and minerals to produce soluble aerosol forms, including UO_3, DU-trioxide (VI).[49] These depleted uranium-oxide products are the dominant species found in areas with depleted uranium penetrator ammunition, and are readily soluble in body fluids.[49, 81]

The type of the mineral particles and organic matter present in an area affects the absorption of environmental metal and its migration from a point-source. Metal contaminant release from soils is limited by the adsorption/desorption rates of individual soil grains. Clay, with a smaller size fraction, will quickly adsorb uranium U(VI) and slowly desorb the metal.[82] Furthermore, migration of existing depleted uranium will also be affected by attenuation reactions, which include “ion exchange and specific adsorption of uranium on organic matter, clay minerals, and ferric oxides and oxyhydroxides commonly present in soil. Under aerobic

conditions, iron can play a key role in controlling the movement through soil. Uranium will bind to many iron minerals and adsorbs to humic matter in the soil. Uptake (complexation) by organic compounds will slow the migration of uranium through soil by several orders of magnitude, so that it becomes essentially immobile."[83]

HAWAI'I MILITARY INSTALLATIONS' USE OF DEPLETED URANIUM

Davy Crockett Weapon System and M101 Spotting Rounds (Non-penetrator, Low-Velocity Munitions)

The U.S. Army deployed depleted uranium launchers to three Hawaiian Island military bases for field training between 1962 and 1968.[84] These non-penetrator 20-mm spotting rounds, known as M101, were ballistically-matched cartridges which used depleted uranium to simulate a penetrator's trajectory path and landing when used in combat. In training maneuvers, the M101 rounds would not impact a hard target which resulted in leaving the outer shells on the surface terrain or up to 8 centimeters (cm) below the surface in specific and limited-access-target areas.[84-86] These non-nuclear M101 projectiles were shot from a 'Davy Crocket' weapon assembly (DCWA). The DCWA was part of the Light Weapon M-28 gun series launcher that were designed to propel either conventional explosives (e.g., TNT) or nuclear (e.g., fission and/or fusion) warheads[87] at the border of East and West Germany during the Cold War period.[84] To realistically simulate the combat experience for effective soldier field practice, the metal incorporated into the spotting rounds was depleted uranium alloyed with 8% molybdenum (^{96}Mo).[88] According to the Munitions Item Disposition Action System (MIDAS) database, the M101 depleted uranium spotting round contained approximately 190 g depleted uranium, within a 20-mm diameter and 190.5-mm-long projectile, which weighed a total of 450

g (~ 1 pound). [84, 89] The nose-cone possessed only a small amount of red phosphorus to generate smoke to visually identify the munition impact point.[7, 90]

A U.S. Army manifest recorded an initial shipment of 714 spotting cartridges from the U.S. manufacturing plant that totaled approximately 135.6 kg (~300 lbs.) of depleted uranium to the Hawai'i Island bases. [91] The quantities distributed to the three different installations was not listed. The DCWA was never used in combat and remained a clandestine classified weapons system until deactivated by the Army in 1968.[87]

In 2005, U.S. Army field inspections identified spotting-round tail assemblies, scraps, and residues on the firing range of Schofield Barracks Military Reservation (SBMR), on O'ahu, Hawai'i. Additional field site investigations on the military firing ranges of Pōhakuloa Training Area (PTA), Big Island Hawai'i discovered similar findings.[7, 87] No evidence of DCWA was found at Mākua Military Reservation (MMR), O'ahu.[92] To comply with U.S. law for the use and/or storage of radioactive material, the U.S. Army requested and was issued a site license in 2013 from the NRC.[93]

The two Hawaiian installations with depleted uranium munition delineated the target shooting area as a 'Surface Danger Area' (SDA) or 'Surface Danger Zone' (SDZ) to restrict and contain vertical and lateral projectile debris. The locations of firing positions were centered 600 m from the SDA edge length and 400-m in width from the fire line, often within an unexploded ordnance (UXO) hazard area. The SDA and SDZ remain designated as a radiological control area (RCA) with access only by escort from explosive ordnance disposal (EOD) staff.[94] The controlled area is 5 percent of the RCA and still used in target training. The base community is 161 m south of the RCA.[84] Ground sweeps, ordnance removal, and other remediation efforts

to remove contamination and restore the landscape are ongoing.[89] Due to the possibility of unexploded ordnance in the SDA, no entry for soil sampling to evaluate uranium isotope levels within the impact areas was permitted for this study. The island areas sampled, with corresponding sample numbers, are shown in Figure 2.2.

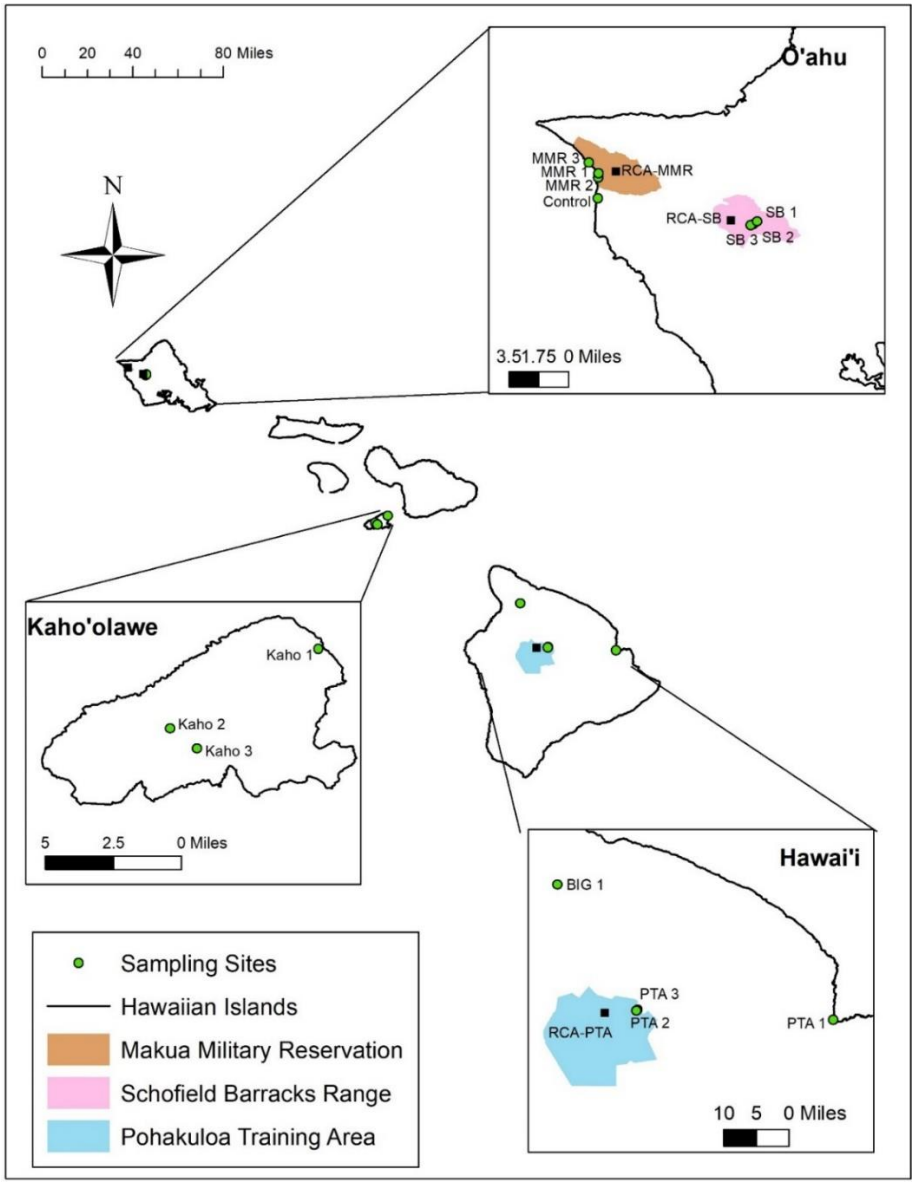

Figure 2.2: The Hawaiian Archipelago, highlighting the 13 soil sample sites, from 3 islands, used in this study of depleted uranium.

Schofield Barracks and Mākua Military Reservation, O'ahu, Hawai'i:

The island of O'ahu is the third largest Hawaiian island and divided into four areas: Schofield Plateau; Wai'anae Range (Forest Reserve) parallels the island's west coast; Ko'olau Range parallels the O'ahu island's east coast; and, the coastal plains.[95] The Schofield Plateau exists in the north-central Wahiawa plateau between two shield volcano ranges.[96] The Schofield Barracks East Range consists of 4,950 acres and is located south of this plateau.[94] The southwest coast of O'ahu is the driest area of the island, including evaporation that can near 50%, during the drier summer months.[97] Northeasterly trade winds have an average speed of 12 knots. The Schofield plateau's southern portion slopes approximately 3 to 5% toward Pearl Harbor (southwest O'ahu).[98]

The Schofield Training area is situated on a total of 1902 hectacres and located in a valley on the east slope of Wai'anae Mountain range, which comprises the west half of O'ahu.[99] The upper northern area of the Schofield Forest Reserve is private land used for pineapple cultivation and adjacent to developed urban areas.[100] Sugarcane fields were once located in the upper portion of the Schofield plateau, but have since been replaced with residential housing and different agricultural activities. The soil from the Schofield Barracks west range was tested in 2000, by U.S. Army contractors (Cabrera Services Inc. (CSI)), for ^{238}U concentrations using gamma spectroscopy analysis. Radiation levels in soils within the restricted munitions site ranged from 0 to 260 Bq/g (0 to 10,404 ppm).[101]

Mākua Military Reservation (MMR) consists of 1942 ha and is 29 km west from Schofield Barracks and positioned on O'ahu's west side. The installation extends from the Wai'anae Range to near the North Shore ocean coast. The Mākua Military Reservation beach has been used for amphibious assault maneuvers by the Marine Corps. Steep cliffs surround the military

impact area and the Army continues frequent live-fire training on the military range. Training logistics includes heavy vehicular traffic (e.g. artillery and tanks) over unpaved roads, along with explosive use on land with little vegetation.

Kaho'olawe, Hawai'i:

Kaho'olawe Island is the smallest of eight main islands of the Hawaiian Archipelago. An Executive Order decreed the entire island for use as an air and sea target range for rocket, bomb, shell, and napalm. President George H.W. Bush permanently ceased the U.S. military bombing on Kaho'olawe Island, and returned the island control to the state of Hawai'i in 1990.[102] There are no records indicating the island was fired upon with depleted uranium armaments. Even so, soil samples from this island were collected to validate this premise.

Pōhakuloa Training Area, Hawai'i:

The largest of the archipelago Hawaiian islands is Hawai'i and is home to Pōhakula Training Area (PTA).[103] The Pōhakuloa Training Area is the U.S. Army's largest installation, consisting of 9,308 hectacres. The Pōhakuloa Training Area lies in a high plateau formed between Mauna Loa (active volcano), Mauna Kea (dormant) and the Hualālai (active) Volcanic Mountains. As early as the late 1950s the Pōhakuloa territory had been used for aerial and land gun training missions by the U.S. military.[104] In 2008, ground and aerial surveys discovered pistons and fragments from the Davy Crocket Weapons Assembly. This area remains in active use and has accommodated company-level , 80 – 250 soldiers and up to nine tanks, and battalion-level, 2 or more companies, during its annual mortar, artillery, and helicopter gun training exercises performed jointly with U.S. Marines.[105] In addition, fixed wing and rotary aircraft participate in this theater of operations using inert munitions and concrete 'dumb'

bombs.[105] On October 23, 2007, B-2 stealth bombers deployed 907 kg bombs onto Pōhakuloa Training Area target areas.[106]

PROCEDURAL METHODS

Soil Collection, Storage, and Preparation for Analysis:

Thirteen soil samples were collected from three Hawai'i islands and labeled according to latitude and longitude coordinates from the iPhone Google Maps Global Positioning System (GPS). Samples were collected from surface to no deeper than 8-centimeter (cm) depths and stored in individual plastic bags or polyethylene conical tubes. The soils were shipped/hand-carried from Hawai'i at ambient temperature and stored at ambient room temperatures prior to testing. Soil was mixed to ensure homogenization, then sieved through a 2 mm opening of a steel mesh screen to provide particle size uniformity and to remove pebbles, sticks, plant roots, or other detritus material. A porcelain mortar and pestle were used to grind the soil to achieve a particle size with increased surface area. The soil sample was heated in a drying oven (100°C) overnight to remove moisture prior to dry weight calculations using a Sartorius Analytic balance (A 200 S), calibrated to ±0.001. The sample weights varied between 0.5 to 0.9 grams (g). The drying step, without sieving, was also applied to the standard reference material (SRM) Montana II soil; National Institute of Standards and Technology (NIST) Standard Reference Material (SRM) 2711a. This Helena, Montana agricultural field soil, recovered by U.S. Geological Survey staff, has 25 certified elements, including uranium. The NIST SRM is a fine-powdered soil processed by sieving through a 74-µm mesh, stored at room temperature, and shipped at room temperature.[107]

Equipment Preparation:

All glassware (100-mL volumetric flasks, funnels, and beakers) were cleaned by soaking in 10% nitric acid (HNO_3) v/v for at least 10 hours, rinsed six times with 18Ω water, then dried in a laminar flow hood. Teflon® beakers, 100-mL capacity, were similarly cleaned and dried. Individual beakers were used for each site's soil sample digestion on hot plates (85°C ± 5°C). Teflon/glass watch-covers over each beaker were used as a vapor recovery (reflux heating) device.

Soil Digestion, Filtration, Dilution:

Soil samples were digested using the EPA approved sample preparation and digestion method #3050B.[108] Reagent grade, concentrated (65%) nitric acid (HNO_3; Fisher Chemical trace metal grade) was used to leach uranium metal from the soil matrix. Soil, 0.5 to 0.9 g, was digested using 5 mL HNO_3 until 3 mL liquid remained. The addition of 1 mL Certified ACS 30% hydrogen peroxide (H_2O_2) was included to remove humic acids from the digestate. Additional 1 mL of H_2O_2 was added until the brown fumes, reaction mixture of nitrogen oxides (nitric acid with oxygen in the air), was absent in the remaining 3 mL digestate.

Digestate samples were cooled to room temperature prior to filtration. Gravitational filtration was used to filter each digested sample. Glass funnels were placed into individual 100-mL volumetric flasks. A single grade-41 Whatman®, ash-less, 90-mm diameter filter paper, was folded in half twice, then wetted with 18Ω H_20. Each folded and wetted filter paper was opened as a cone, then pressed firmly to fit against the individual funnels. The ~3mL of digested sample was transferred to the volumetric flask setup through the filter. The remaining precipitate in the beaker was rinsed with 18Ω H_2O three times and poured over the filter paper. Finally, 1 mL of

18Ω H_2O was added to rinse the filter and wash down the filter paper. Upon complete liquid filtration, the funnel set-up was removed. Samples were diluted to 100mL final volume using 18Ω H_2O.

Duplicate samples were processed to monitor reproducibility of the method. Recovery precision of uranium isotopes from acid digestion was evaluated using – Montana II soil, SRM# 2711a, Lot # 2009.[107]

Digested and solubilized soil samples were stored in 3 % HNO_3 to retard biological and chemical reactions. Also, the inclusion of nitric acid reduces the formation and precipitation of hydroxides or other metal complexes that may form with other molecules or ions dissolved in the digested solution.[109]

Purchased uranium ICP standard, from Ricca® Chemical Company, (1 ml = 1000 ppm U) in 3% HNO_3, Lot No. 4510A19 (NIST SRM 3164), expiration date Apr, 2017, was used as external calibration standards for Hawai'i soil analysis. The calibration standards were prepared using dilutions of the working standard (1000 ppm uranium). Standard concentrations of 0.5, 1.0, 5.0, 10.0, 25.0, 50.0, 100.0 ppb were prepared using 3% as HNO_3 the diluent. A matrix sample was prepared by spiking an analyzed soil sample with a known addition of uranium to recover $^{235}U/^{238}U$ ratios. No Certified Reference Material (CRM) was used to validate the isotopic ratios reported in the analysis by ICP-MS. The uranium calibration standards were used to test for isotope ratio consistency during all analytical runs.

Analysis was performed according to EPA Method 200.8 (Revision 5.4).[110] The bench-top ICP-MS instrument, Perkin-Elmer Elan DRC-e NexIon® 1000 and auto-sampler, analyzed all digested samples. Liquid Argon (Ar), 675 - 725 kPa, was used as the carrier gas at 0.8 – 1.3 L/min

to transport the analyte species to the mass spectrometer. This controls the sample liquid nebulization efficiency, minimizing oxide formation. A platinum cone and a Ryton Scott spray chamber were used. The NexIon uses the Elan Software. The SmartTune solution was purchased from Perkin-Elmer and contained 1% HNO_3 with Ba, Be, Ce, Co, In, Pb, Mg, Rh, and U per 1000 mL. Terbium (^{170}Tb) was used as the internal standard (IS). A radio frequency power of 1100W was used to maximize the sensitivity of identifying uranium isotopes. Each digested sample was analyzed three times to acquire three points per uranium isotope mass, with 30 sweeps per reading. A dwell time of 500 ms was used to ensure full passage of one sample prior to testing a follow-up sample. The Elan elemental resolution is 0.698 $\pm$ 0.1 amu.

RESULTS

The 13 sites were analyzed for the counts per second (CPS) of the two uranium isotopes. Multiple analyses of the samples were performed to determine standard deviation in the instrument analyses . An alpha value of 0.05 was used for all statistical tests. The site's ratio values, standard deviations (repeatability standard error percent), and percent difference from the theoretical value of 0.007257 are listed in Table 2. A one-way analysis of variance showed that there was no significant difference (p=0.18) between the 13 sites in relation to the $^{235}U/^{238}U$ ratios, however this information is not of use in point source data discussion. The graph with error bars, Figures 3-6, indicate the 95% confidence interval using one standard error mean for each soil area.

The quality control of total uranium analyzed for $^{235}U/^{238}U$ isotope ratio abundances yielded 0.0073 for 1, 10, 50, and 100 ppb levels; standard deviation of 0.00007. The standard reference material (SRM) for $^{235}U/^{238}U$ ratio yielded 0.0073; standard deviation of 0.00005.

Table 2.2: Kaho'olawe (Kaho) collection sites 1-3; Mākua Military Reservation (MMR) collection sites 1-3; Schofield Barracks (SB) collection sites 1-3; Pōhakuloa Training Area (PTA) collection sites 1-3; Big Island (Big 1) collection site.

Sample #	***U^{235}/U^{238}***	***Std error %***	***% Difference from theoretical***	***Final ^{235}U [ppm] calc***	***Final ^{238}U [ppm] calc***	***Island/Site name***
Kaho 1	7.362×10^{-3}	0.0023	1%	0.004	0.58	Hakio'awa; largest early settlement (NE of island)
Kaho 2	7.394×10^{-3}	0.0032	2%	0.01	1.6	Above Hakio'awa
Kaho 3	7.316×10^{-3}	0.0042	1%	0.008	1.1	Center of Kaho'olawe
MMR 1	7.273×10^{-3}	0.0014	0.2%	0.002	0.03	MMR; 11.8 km from MMR-RCA
MMR 2	7.228×10^{-3}	0.0042	-0.4%	0.004	0.52	MMR; 12.1 km from MMR-RCA
MMR 3	7.390×10^{-3}	0.0012	2%	0.004	0.58	MMR; 12.9 km from MMR-RCA
SB 1	7.331×10^{-3}	0.0003	1%	0.002	0.33	2 km to SB-RCA
SB 2	7.303×10^{-3}	0.0003	1%	0.006	0.84	2 km to SB-RCA
SB 3	7.228×10^{-3}	0.0004	0.4%	0.002	0.24	2 km to SB-RCA
PTA 1	7.361×10^{-3}	0.0017	1%	0.008	1.2	53 km from PTA-RCA
PTA 2	7.399×10^{-3}	0.0007	2%	0.002	0.3	Mauna Kea State Park; 7.7 km to PTA-RCA
PTA 3	7.333×10^{-3}	0.0018	1%	0.003	0.5	Hilo; 7 km to PTA-RCA
BIG 1	7.409×10^{-3}	0.0020	2%	0.004	0.5	Waimea; 33.5 km to PTA-RCA

*RCA: Radiation Control

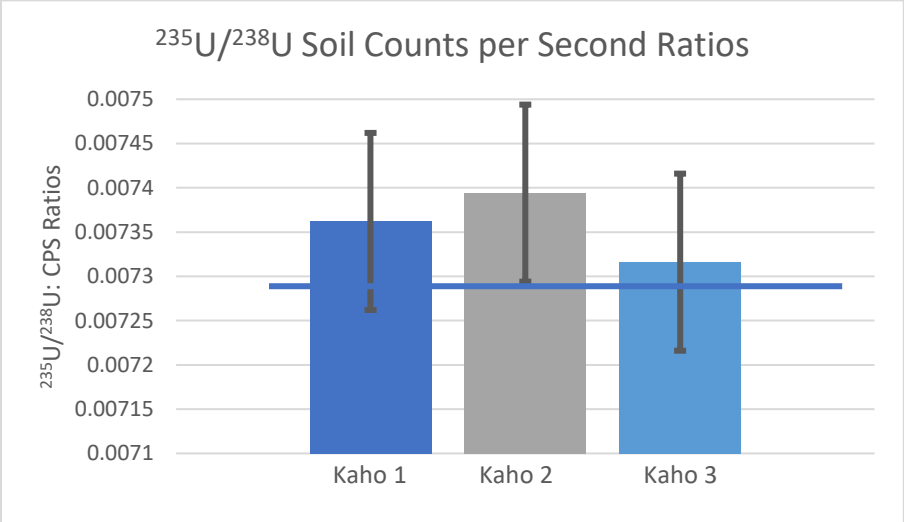

Figure 2.3: Soil uranium counts per second (CPS) isotope ratios for Kaho'olawe (Kaho 1-3). Error bars indicate 95% confidence intervals of each sample site using one standard error. Solid horizontal line indicates theoretical uranium ratio value (0.007257).

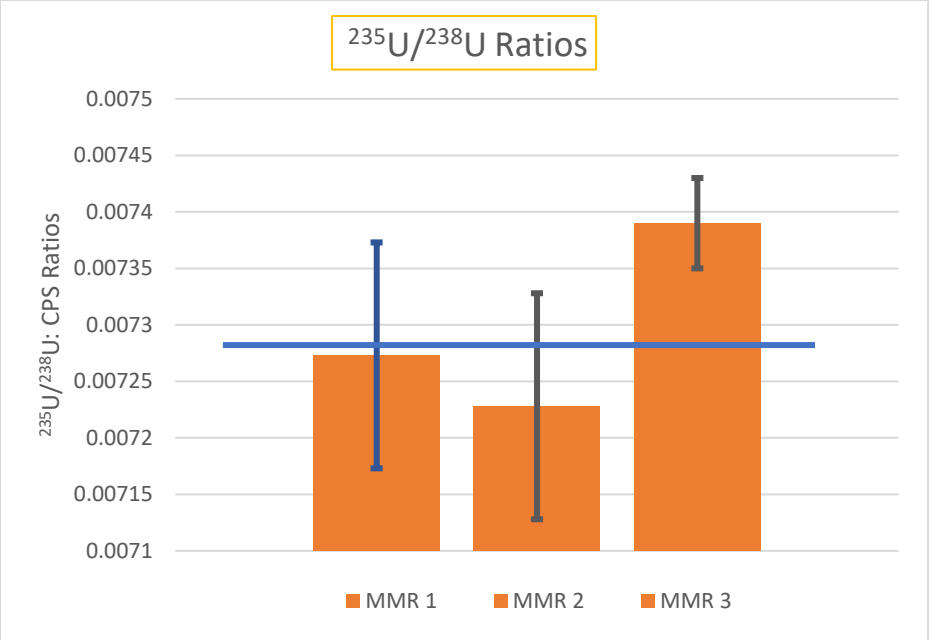

Figure 2.4: Mākua Military Reservation (MMR); uranium isotopes ($^{235}U/^{238}U$) counts per second (CPS) ratios. Error bars indicate 95% confidence intervals of each soil point source using one standard error.

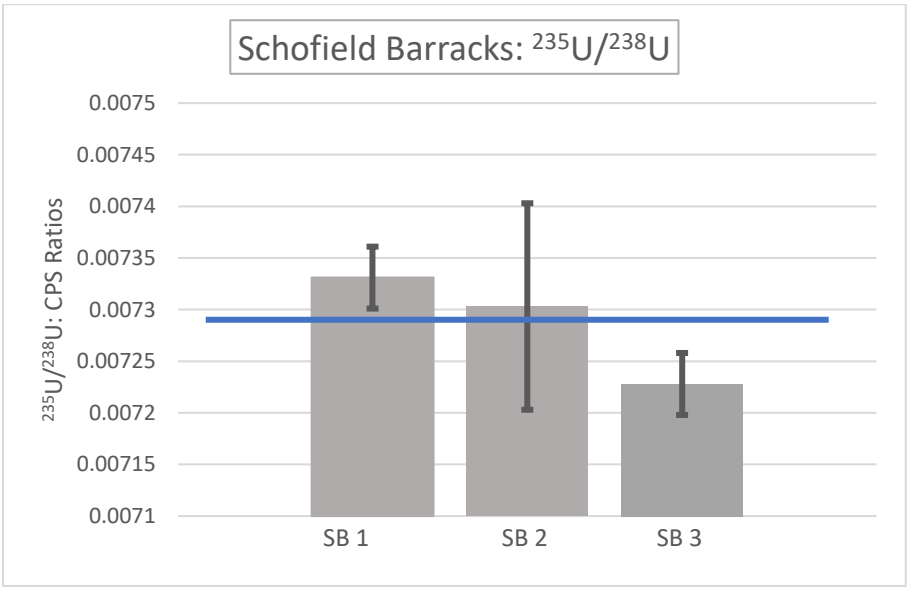

Figure 2.5: Schofield Barracks site collections (SB 1-3). Uranium soil isotope ratios $^{235}U/^{238}U$. Error bars indicate 95% confidence intervals of each site using one standard error. Solid horizontal line indicates theoretical uranium ratio abundance value (0.007257).

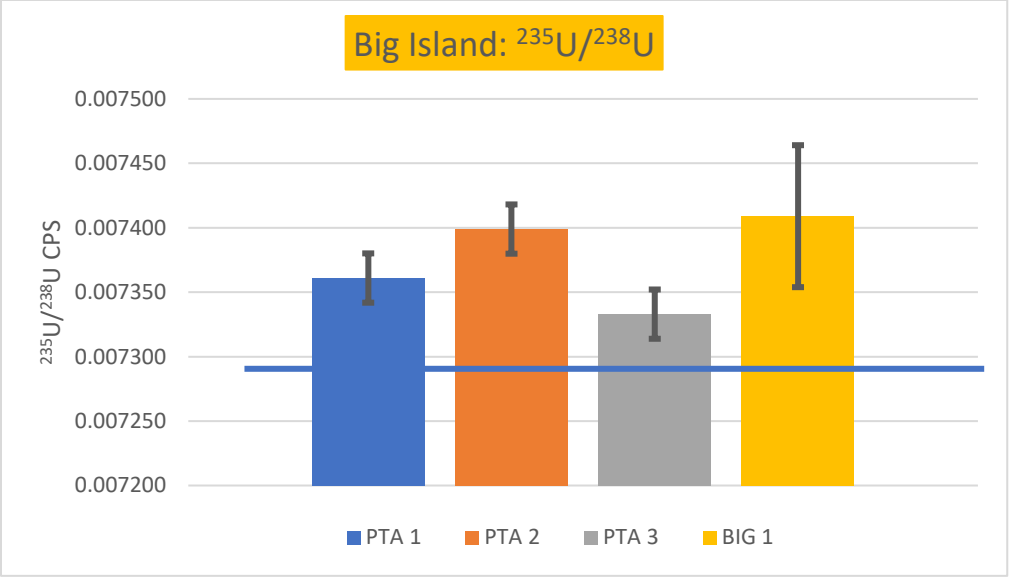

Figure 2.6: Soil uranium isotope ratios for Pōhakuloa Training Area sites (PTA 1-3) and Waimea (BIG 1), north of the PTA perimeter. Error bars indicate 95% confidence intervals of each point source using one standard error. Solid horizontal line represents the theoretical uranium ratio value of 0.007257.

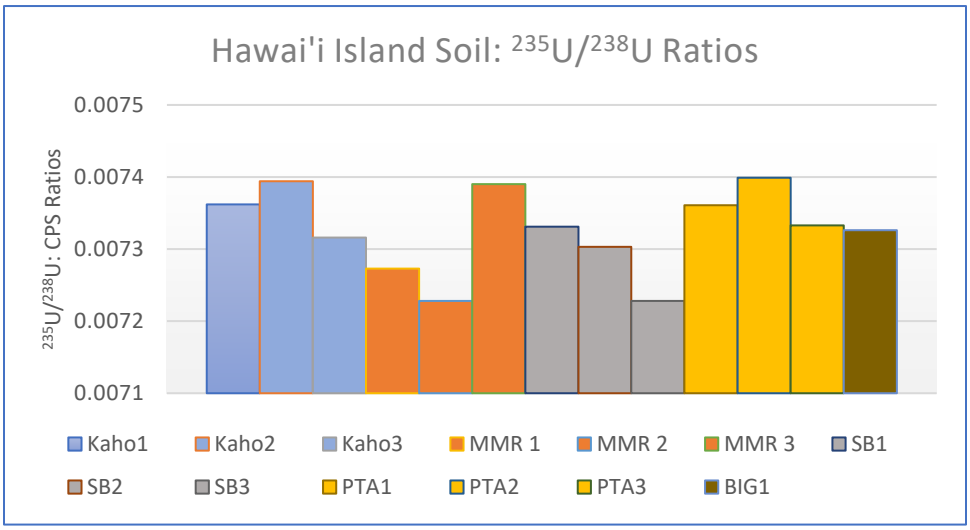

Figure 2.7: Comparison of the 13 point-sources collected for $^{235}U/^{238}U$ ratios on the Hawai'i Islands

DISCUSSION

This study examined the isotope ratios of $^{235}U/^{238}U$ to detect abundance of ^{238}U above background levels of natural uranium (NU) that exist in soil from weathered rock. The ICP-MS counts-per-second (CPS) were used in ratio calculations for all collected soil analyses. The dry mass weight of total ^{238}U to determine parts per million (ppm) was not used as a criteria for point source analysis due to the natural levels existing in the area, approximately 0.2 – 2.0 ppm in uncontaminated basalt.[111]

Soil collection sites close to Schofield Barracks Radiation Control Area (SB RCA, Table 2.2), approximately 2 km, were rocky or consisted of small mixtures of red-colored soil/organic matter. Uranium may have become imbedded below the surface of the uneven training terrain on Schofield Barracks, or in 'pockets' between the rocky surfaces and the surrounding forest. Also, the Schofield Barracks firing ranges continue to be occupied with live small-arm fire exercises, even during the time of our soil collection, which limited the scope of soil collection needed for improved characterization of the region.

Using the ICP-MS isotope analysis, 1-2% difference in $^{235}U/^{238}U$ abundance was detected, from the theoretical value of 0.007257, in three point-source collection areas. This small percentage is considered within the experimental uncertainty, rather than any migration evidence. This self-funded study yielded a small number of sampling site collection points, none closer than 2 km to the predicted center of an RCA on each military installation firing range. Apparent from this study is that finding lower natural abundance uranium ratios will require additional soil collection, more formally in a grid matrix. Also, absence of lowered natural isotope abundance is likely due to weather events that may have mobilized and equilibrated

isotope ratios in the soil we were able to access. Ground water levels were not tested during this study, nor was any foliage. Tree bark in neighboring forest reserves may provide air quality information on depleted uranium burden that exists in the vicinity of the radiation control zone of the two islands that used depleted uranium spotter rounds.[112] Testing lichen biota, which lack roots, may measure accumulated airborne uranium that hasn't washed away from weather events over the fifty years after the arsenal was removed from use.[113]

The soil results from three areas of the Kaho'olawe Island, two from the upper mountain range and one from the coastal region, confirmed no evidence of excess depleted uranium presence. The depleted uranium soil testing results, calculated from the $^{235}U/^{238}U$ isotope ratio counts using ICP-MS, of this island were within 1 SD of the analyzed isotope ratios of the other islands.

CONCLUSION

To assess depleted uranium migration away from three Hawai'i military base firing impact areas, also known as Radiation Control Areas (RCA), $^{235}U/^{238}U$ soil ratios were compared to the theoretical natural abundance value. Even though Hawai'i has a natural uranium background small differences were found even with the small number of samples collected. These 1-2% differences can be attributed to experimental uncertainty in soil size selection, digestion, and dilution procedures. Future study considerations would include greater soil sample numbers, utilizing a grid design in areas closer to the RCA. Gradient distance sampling is also recommended of the military base forest range that surrounds the impact area perimeter as well as downhill toward the surrounding residential areas. The diverse terrain and isolating

forested areas are likely to have collection pockets that have retained a source of depleted uranium undetected by the current study due to area access restrictions. Moreover, sampling of area tree bark or lichen could also provide insight to accumulated levels of airborne depleted uranium over the past 50 years. [112, 113]

REFERENCES

1. Chem.libretexts.org. *General Properties and Reactions of the Actinides*. 2017 August 21, 2017 [cited 2018 November 13, 2018]; Available from: read: https://chem.libretexts.org/Textbook_Maps/Inorganic_Chemistry/Supplemental_Modules_(Inorganic_Chemistry)/Descriptive_Chemistry/Elements_Organized_by_Block/4_fBlock_Elements/The_Actinides/1General_Properties_and_Reactions_of_The_Actinides.
2. Abu-Qare, A.W. and M.B. Abou-Donia, *Depleted Uranium--The Growing Concern.* Journal of Applied Toxicology, 2002. **22**(3): p. 149-52.
3. Argonne National Lab, E., *Depleted Uranium*, U.S. Department of Energy, Editor. 2005, ANL: Argonne, Illinois. p. 1-4.
4. Army, *Depleted Uranium - Medical*. 2016, U.S. Army Medical Department: Aberdeen Proving Ground, Maryland 21010-5403.
5. Arzuaga, X., et al, *Modes of Action Associated with Uranium Induced Adverse Effects in Bone Function and Development.* Toxicology Letters, 2015. **236**: p. 123-130.
6. UEC, *Technical Report For Uranium Energy Corp Salvo Project In-Situ Recovery Uranium Property Bee County, Texas*. 2011, United Energy Corp: Corpus Christi, TX. p. 55.
7. ATSDR, *Health Consultation: Depleted Uranium at Hawai'ian Military Sites; Schofield Barracks Impact Area, Makua Military Reservation, Pohakuloa Training Area on Islands of O'ahu and Hawai'i*, HHS, Editor. 2008, ATSDR: Atlanta, GA 30333.
8. Leggett, R.W., *Biokinetics of Uranium in the Human Body*, in *Depleted Uranium, Properties, Uses, and Health Consequences*, A. Miller, Editor. 2007, CRC Press: New York, NY. p. 163-182.
9. Eckerd, J., *Insights in public health: the facts about depleted uranium in Hawai'i.* Hawaii J Med Public Health, 2013. **72**(11): p. 404-5.
10. Emsley, J., *The Elements*. 3 ed.: Oxford Press.
11. Goldstein, S.J., Rodriguez, J.M., Lujan, N. , *Measurement and Application of Uranium Isotopes for Human and Environmental Monitoring.* Health Physics, 1997. **72**(1).
12. Brennecka, G.A., et al, *Natural Variations in Uranium Isotope Ratios of Uranium Ore Concentrates: Understanding the 238U/235U Fractionation Mechanism.* Earth and Planetary Science Letters, 2010. **291**(1-4): p. 228-233.
13. Richter, S., et al., *The Isotopic Composition of Natural Uranium Samples.* International Journal of Mass Spectrometry, 2008. **269**(1-2): p. 145-148.
14. Giraldo, J.S., Gotham, Douglas J., Nderitu, David G., Preckel, Paul V., Mize, Darla J., *Fundamentals of Nuclear Power*. 2012.
15. Craft, E., et al., *Depleted and Natural Uranium: Chemistry and Toxicological Effects.* Journal of Toxicology and Environmental Health, Part B Critical Reviews, 2004. **7**(4): p. 297-317.
16. NRC. 2018 April 23, 2018 [cited 2018 June 15, 2018]; Available from: https://www.nrc.gov/reading-rm/basic-ref/glossary/depleted-uranium.html.
17. Fujikawa, Y., et al, *Variation in Uranium Isotopic Ratios 234 U/238U and 235U/total-U in Japanese Soil and Water Samples —Application to Environmental Monitoring*, in *10th International Congress of the International Radiation Protection Association*. 2000, Japan Health Physics Society: Hiroshima, Japan. p. 1-6.

18. Magnoni, M., et al, *Variations Of the Isotopic Ratios Of Uranium In Environmental Samples Containing Traces Of Depleted Uranium: Theoretical and Experimental Aspects.* Radiation Protection Dosimetry, 2001. **97**(4): p. 337-340.
19. Condon, D.J., et al, *Isotopic Composition (238U/235U) of Some Commonly Used Uranum Reference Materials.*
20. Fujii, Y., et al, *Anomalous Isotope Fractionation in Uranium Enrichment Process.* Journa of Nuclear Science and Technology, 1989. **26**(11): p. 1061-1064.
21. UNEP, *Post-Conflict Environmental Assessment*, in *Depleted Uranium in Kosovo*. 2001, United Nations.
22. Sheppard, S.C., et al, *Critical Compilation and Review of Plant/Soil Concentration Ratios for Uranium, Thorium and Lead.* Journal of Environmental Radioactivity, 1988. **8**: p. 255-285.
23. Laurette, J., et al, *Speciation of Uranium In Plants Upon Root Accumulation and Root-To-Shoot Translocation: A XAS and TEM Study.* Environmental and Experimenal Botany, 2012. **77**: p. 87-95.
24. Yoshida, S., et al., *Concentrations of Uranium and 235U/238U Ratios in Soil and Plant Samples Collected Around the Uranium Conversion Building in the JCO Campus.* Journal of Environmental Radioactivity, 2000. **50**(1–2): p. 161-172.
25. EPA, *Depleted Uranium Technical Brief*, B. Littleton, Editor. 2006.
26. ATSDR, in *Toxicological Profile for Uranium*. 2013. p. 11-37.
27. WHO, *Depleted Uranium Sources, Exposure and Health Effects*, in *Industrial, Commercial and Military Applications*, WHO, Editor. 2001, World Health Organization: Geneva, Switzerland.
28. Konietzka, R., *Gastrointestinal Absorption of Uranium Compounds - A Review.* Regulatory Toxicology and Pharmacology, 2015. **71**: p. 125-133.
29. EPA, *Radionuclides Rule: A Quick Reference Guide*, in *EPA 816-F-01-003*, E.P. Agency, Editor. 2001: Washington, D.C. p. 1-2.
30. WHO, *Uranium in Drinking-Water, Background document for development of WHO Guidelines for Drinking-Water Quality*. 2012, WHO Press.
31. ATSDR, *Toxicological Profile for Uranium*, HHS, Editor. 2013, Federal Registry: Atlanta, GA 30333. p. 1-526.
32. Burkart, W., P.R. Danesi, and J.H. Hendry, *Properties, Use and Health Effects of Depleted Uranium.* International Congress Series, 2005. **1276**: p. 133-136.
33. McLaughlin, J.P., Waligorski, Michael P. R., *Depleted Uranium - A Health, Environmental or Societal Issue.* Archive of Oncology, 2001. **9**(4): p. 213-4.
34. Mould, R.F., *Depleted Uranium and Radiation-Induced Lung Cancer and Leukaemia.* The British Journal of Radiology, 2001. **74**(884): p. 677-683.
35. Vicente, L., et al, *Nephrotoxicity of Uranium: Pathophysiological, Diagnostic and Therapeutic Perspectives.* Toxicological Sciences, 2010. **118**(2): p. 324-347.
36. Parrish, R.R., et al, *Depleted Uranium Contamination by Inhalation Exposure and Its Detection After ~20 years: Implications for Human Health Assessment.* Science of The Total Environment, 2008. **390**(1): p. 58-68.
37. World-Health-Organization, *Health Effects of Depleted Uranium; Report by the Secretariat*. 2001.

38. Boeing, *Boeing Use of Depleted Uranium Counterweights in Aircraft*, NRC, Editor. 1994, Boeing Company: Seattle, WA.
39. Betti, M., *Civil Use of Depleted Uranium.* Journal of Environmental Radioactivity, 2001. **64**: p. 113-119.
40. DOE, *Depleted Uranium: A DOE Management Challenge*. 1995, U.S. Department of Energy, Office of Environmental Management, Office of Technology Development: Oak Ridge, TN 37831.
41. Usov, I.S., Milan, *Uranium Oxide Solar Cells*, in *US Patent Application Publication*, L. Los Alamos National Security, Editor. 2017, Los Alamos National Security, LLC: USA. p. 6.
42. Davitt, R.P., *Depleted Uranium and Tungsten Alloy as Penetrator Materials*. Jun, 1980, US Army: US Army Armament Research and Development Cmmand; Dover, NJ 07801. p. 32.
43. Bradley, C.E., Jr., *The Future For Beneficial Uses Of Depleted Uranium*. 2003. p. 1-11.
44. Lemons, T.R. *The Ultimate Disposition of Depleted Uranium*. in *Second International Conference Uranium Hexafluoride Handling*. 1992. Oak Ridge, TN.
45. Hong, S.H., et al, *Combination of Mechanical Alloying and Two-Stage Sintering of a 93W-5.6Ni-1.4Fe Tungsten Heavy Alloy.* Materials Science and Engineering, 2002. **A3444**: p. 253-260.
46. GAO, *Gulf War Illnesses Understanding Of Health Effects From Depleted Uranium Evolving but Safety Training Needed*, in *Depleted Uranium Health Effects*. 2000, National Security and Internation Affairs Division.
47. Hamilton, E.I., *Depleted Uranium (DU): A holistic Consideration of DU and Related Matters.* Science of The Total Environment, 2001. **281**(1-3): p. 5-21.
48. NRC, *Review of Toxicologic and Radiologic Risks to Military Personnel From Exposure to Depleted Uranium During and After Combat*. 2008: Washington, DC.
49. Katz, S.A., *The Chemistry and Toxicology of Depleted Uranium.* Toxics, 2014. **2**: p. 50-78.
50. Bem, H., Bou-Rabee, Firyal, *Environmental and Health Consequences of Depleted Uranium in the 1991 Gulf War.* Environment International, 2004. **30**: p. 123-134.
51. Bleise, A., P.R. Danesi, and W. Burkart, *Properties, Use and Health Effects of Depleted Uranium (DU): A General Overview.* J Environ Radioact, 2003. **64**(2-3): p. 93-112.
52. Roszell, L.E., et al., *Assessing the renal toxicity of Capstone depleted uranium oxides and other uranium compounds.* Health Phys, 2009. **96**(3): p. 343-51.
53. Brown, J.S., et al, *Thoracic and Respirable Particle Definitions for Human Health Risk Assessment.* Particle and Fibre Toxicology, 2013.
54. Di Lella, L.A., et al, *Uranium Contents and (235)U/(238)U Atom Ratios in Soil and Earthworms in Western Kosovo After the 1999 War.* Science of the Total Environment, 2005. **337**(1-3): p. 109-118.
55. Durante, M. and M. Pugliese, *Depleted Uranium Residual Radiological Risk Assessment for Kosovo Sites.* Journal of Environmental Radioactivity, 2003. **64**(2-3): p. 237-45.
56. Uyttenhove, J., M. Lemmens, and M. Zizi, *Depleted Uranium in Kosovo: Results of a Survey by Gamma Spectrometry on Soil Samples.* Health Phys, 2002. **83**(4): p. 543-8.
57. Jia, G., et al., *Concentration and Characteristics of Depleted Uranium in Biological and Water Samples Collected in Bosnia and Herzegovina.* Journal of Environmental Radioactivity, 2006. **89**(2): p. 172-87.

58. UNEP, *Depleted Uranium in Bosnia and Herzegovina, Post Conflict Environmental Assessment Report*. 2003: Switzerland.
59. WHO, *Depleted Uranium: Sources, Exposure and Health Effects - Executive Summary*. 2001, WHO: Geneva, Switzerland.
60. USAF, *Depleted Uranium Fact Sheet*. 1998.
61. Programme, U.N.E., *Lebanon, Post-Conflict Environmental Assessment*. 2007, United Nations: Geneva, Switzerland. p. 184.
62. *Depleted Uranium - Medical*, H.P. Program, Editor. 2016, U.S. Army Public Health Center: Aberdeen Proving Ground, Maryland 21010-5403. p. 2.
63. Mitsakou, C., et al., *Modeling of the dispersion of depleted uranium aerosol.* Health Phys, 2003. **84**(4): p. 538-44.
64. Török, S., et al., *Characterization and Speciation of Depleted Uranium in Individual Soil Particles Using Microanalytical Methods.* Spectrochimica Acta Part B: Atomic Spectroscopy, 2004. **59**(5): p. 689-699.
65. Todorov, T.I., et al, *Depleted Uranium: Properties, Uses, and Health Consequences*, ed. C.M. Alexandra. 2006, Boca Raton, FL 33487: CRC Press. 1-259.
66. EPA, U.S., *User's Guide: Radionuclide Carcinogenicity.* 2015.
67. Calabrese, E.J., *The Emergence of the Dose–Response Concept in Biology and Medicine.* International Journal of Molecular Sciences, 2016. **17**(2034): p. 1-14.
68. Durakovic, A., *Medical effects of internal contamination with uranium.* Croat Med J, 1999. **40**(1): p. 49-66.
69. Canu, I.G., et al, *Cancer Risk in Nuclear Workers Occupationally Exposed to Uranium - Emphasis on Internal Exposure.* Health Physics, 2008. **94**(1): p. 1-17.
70. Wise, S.S., et al, *Particulate Depleted Uranium Is Cytotoxic and Clastogenic to Human Lung Cells.* Chem Res Toxicol, 2007. **20**: p. 815-820.
71. Rouas, C., et al, *Distribution of Soluble Uranium in the Nuclear Cell Compartment at Subtoxic Concentrations.* Chemical Research in Toxicology, 2010. **23**(12): p. 1883-1889.
72. NRC. *Radiation Basics*. 2014 October 17, 2014; Available from: https://www.nrc.gov/about-nrc/radiation/health-effects/radiation-basics.html.
73. Karpas, Z., et al, *Uranium in urine--normalization to creatinine.* Health Physics, 1996. **74**(1): p. 86-90.
74. Shelley, R., et al, *Uranium Associations with Kidney Outcomes Vary by Urine Concentration Adjustment Method.* Journal of Exposure Science and Environmental Epidemiology, 2014. **24**(1): p. 58-64.
75. McDiarmid, M.A., et al, *The U.S. Department of Veterans' Affairs Depleted Uranium Exposed Cohort at 25 Years: Longitudinal Surveillance Results.* Environmental Research, 2017. **152**: p. 175-184.
76. VA, *Gulf War Illness and the Health of Gulf War Veterans: Research Update and Recommendations, 2009-2013*. 2014, S. Government Printing Office: Washington, D.C.
77. Priest, N.D., *Toxicity of Depleted Uranium.* Lancet, 2001. **357**(9252): p. 244-6.
78. McDiarmid, M.A., et al., *Biologic Monitoring and Surveillance Results for the Department of Veterans Affairs' Depleted Uranium Cohort: Lessons Learned from Sustained Exposure Over Two Decades.* American Journal of Industrial Medicine, 2015. **58**(6): p. 583-94.
79. Squibb, K.S. and M.A. McDiarmid, *Depleted uranium exposure and health effects in Gulf War veterans.* Philos Trans R Soc Lond B Biol Sci, 2006. **361**(1468): p. 639-48.

80. Milacic, S., et al., *Examination of the Health Status of Populations from Depleted-Uranium-Contaminated Regions.* Environmental Research, 2004. **95**(1): p. 2-10.
81. Hon, Z., Österreicher, Jan, Navrátil, Leoš, *Depleted Uranium and Its Effects on Humans.* Sustainability, 2015. **7**: p. 4063-4077.
82. Shang, J., et al, *Effect of Grain Sizes on Uranium (VI) Adsorption/Desorption Kinetics and Rate Additivity.* 2010.
83. SCHER, *Opinion on the Environmental and Health Risks Posed by Depleted Uranium*, in *Health & Consumer Protection*, S.C.o.H.a.E. Risks, Editor. 2010, European Commission. p. 41.
84. USACE, *Archive Search Report On the Use of Cartridge, 20 mm Spotting M101 For Davy Crockett Light Weapon M28*, in *Schofield Barracks and Associated Training Areas Islands of Oahu and Hawaii*. 2007, USACE: St. Louis, MO. p. 1-508.
85. Cabrera, S., *Technical Memorandum For Pohakuloa Training Area (PTA) Aerial Surveys The Big Island (Hawai'i), Hawai'i*. 2009: East Hartford, CT. p. 65.
86. Hawaii-State-Health-Department and *The Facts About Depleted Uranium In Hawaii*. 2013. p. 1-4.
87. NRC, *US Army Decommissioning Funding Plan Davy Crockett M101 Depleted Uranium Impact Areas License SUC-1593*. 2015. p. 1-18.
88. Army, *Safety Evaluation Report: for the U.S. Army's Possession License for Depleted Uranium from the M101 Spotting Round*. 2013, U.S. Nuclear Regulatory Commission. p. 1-43.
89. NRC, *Safety Evaluation Report For the U.S. Army's Possession License for Depleted Uranium from Davy Crockett M101 Spotting Rounds – Amendment to Add Remaining Sites*. 2016. p. 82.
90. Army, *3.11 Hazardous Materials and Waste*, in *Supplemental Draft Environmental Impact Statement*. 2008. p. 3_324-347.
91. NRC, *Nuclear Regulatory Commission Issuances*. 2010: Washington, D.C. p. 706.
92. Army, *Final Environmental Impact Statement Military Training Activities at Makua Military Reservation, Hawai'i*. 2009. p. 1-1000.
93. NRC, *License For Depleted Uranium at U.S. Army Sites*, in *Backgrounder*, O.o.P. Affairs, Editor. 2016, Nuclear Regulatory Commission: Washington, D.C.
94. Army, *Site-Specific Environmental Radiation Monitoring Plan Schofield Barracks Military Reservation, Oahu, Hawaii Annex 18*, in *For Materials License SUC-1593, Docket No. 040-09083*. 2016, Installation Management Command: Houston, Texas 78234-1223.
95. Visher, F.N., et al, *Ground-Water Resources in Southern O'ahu, Hawai'i*, in *Geological Survey Water-Supply*, USGS, Editor. 1964: Washington, D.C. p. 144.
96. Hibbard, D., J., *Schofield Barracks Military Reservation, Haer No. Hi-81 Ku Tree Reservoir*. 2008. p. 20.
97. Giambelluca, T.W., et al, *Water Balance, Climate Change and Land-Use Planning in the Pearl Harbor Basin, Hawai'i*, in *Water Resources Development*. 1996, Department of Geography, University of Hawai'i at Manoa: Honolulu, Hawai'i. p. 515-530.
98. Shade, P.J., et al, *Water Budget and the Effects of Land-Use Changes on Ground-Water Recharge, O'ahu, Hawai'i*, ed. W.D. Nichols. 1996, Denver, CO 80225: USGS.
99. MIlitarybases.com. *Schofield Barracks Army Base in Oahu, HI*. 2000; Available from: https://militarybases.com/schofield-barracks-army-base-in-oahi-hi/.

100. Army, *Land Use/Recreation*. 2003. p. 5.2 - 5.34.
101. Army, U., *Environmental Radiation Monitoring Plan For Schofield Barracks Wahiawa, Hawaii, FINAL*, U.S.A.C.o. Engineers, Editor. 2011, Environmental and Munitions Design Center: Baltimore, MD.
102. Commission, K.o.I.R., *Kaho'olawe Island Reserve FY14 Year-In-Review*, M.K. Nāhoʻopiʻ, Editor. 2014.
103. NPS. *Hawai'i Volcanoes*. National Park Hawai'i 2013 June 5, 2013 [cited 2018 1 August 2018]; Available from: https://www.nps.gov/havo/faqs.htm.
104. Commission, U.N.-R., *Safety Evaluation Report For the U.S. Army's Possession License for Depleted Uranium from the M101 Spotting Round*. 2013, Office of Federal and State Materials and Environmental Management Programs: U.S. Army Installation Management Command. p. 43.
105. USMC, *Construction of an Urban Close Air Support Range and an Aviation Bulls-Eye Range at Pohakuloa Training Area, Hawai'i*. 2013, U.S. Marine Corps: HI. p. 117.
106. Wilson, S. *B-2s Train with JTACs, Drop Bombs on Training Range*. 2007 October 29, 2007 [cited 2018 June 22, 2018]; Available from: http://www.pacaf.af.mil/News/Article-Display/Article/596708/b-2s-train-with-jtacs-drop-bombs-on-training-range/.
107. NIST, *Certificate of Analysis Standard Reference Material 2711a Montana II Soil*. 2009.
108. EPA, *Sample Preparation Method 3050B, Revision 2*, in *Acid Digestion of Sediments, Sludges, and Soils*. 1996, EPA: Washington, D.C. p. 1-12.
109. EPA, *Methods for Chemical Analysis of Water and Wastes*, in *Sample Preservation*. 1983, EPA: Cincinnati, OH.
110. EPA, *Determination of Trace Elements In Waters AND Wastes By Inductively Coupled Plasma - Mass Spectrometry*. 1994: Washington, DC.
111. Rubin, K.H., *Depleted Uranium, Natural Uranium and Other Naturally Occurring Radioactive Elements in Hawai'ian Environments*. 2008.
112. Bellis, D., et al, *Airborne Uranium Contamination — as Revealed Through Elemental and isotopic Analysis of Tree Bark.* Environmental Pollution, 2001. **2001**: p. 383-387.
113. Di Lella, L.A., et al, *Lichens as Biomonitors of Uranium and Other Trace Elements in an Area of Kosovo Heavily Shelled with Depleted Uranium Rounds.* Atmospheric Environment, 2003. **37**(38): p. 5445-5449.

CHAPTER III

UPDATE TO THE EPA TEXAS STATE RADON MAP

(**under review for publication to Journal of Environmental Radioactivity**)

ABSTRACT

Radon is a natural source of indoor air pollution that can exist in residences and enclosed buildings with reduced air exchange rates. Areas of the United States with potentially high indoor radon levels are documented via an Environmental Protection Agency (EPA) indoor radon map created circa 1990. Our compilation of > 32,000 Texas homes' data points, collected between 2001 to 2018, has revealed the existence of areas that exceed the recommended indoor health levels of radon. This map update will be given widespread publication to communicate the high radon findings across many Texas counties. Since exposure to radon in homes is a contributing factor to lung cancer, the study's radon data will endorse new state policies governing construction using gas impermeable materials beneath the building foundation in affected areas.

INTRODUCTION

In 1980, the United State of America Environmental Protection Agency (EPA) ranked radon gas a carcinogen and "the most considerable environmental threat to the health of the community".[1] The U.S. Congress added an 'Indoor Radon Abatement' statute to the Toxic Substances Control Act (TSCA) of 1976[2] to facilitate the mitigation of unsafe radon exposure levels in federal facilities. This indoor exposure is in addition to the radiation we all experience

from the ground environment known as Naturally Occurring Radioactive Materials (NORM).[3] Chronic exposure to high indoor radon levels is linked to impaired respiratory health,[4] the leading cause of lung cancer for nonsmokers,[5-7] and an increased cancer risk to tobacco smokers.[8]

The State of Texas covers 696,200 km^2, and is ranked the second-largest U.S. state, after Alaska.[9] Regional climates vary from the continental high plains that consist of extended droughts, to southern marine/subtropical regions that average low rainfalls in winter.[10] The mountain-type cold winters in the north and west transition from the hilly and flat lands of the Rolling Plains to the high elevations of the Caprock Escarpment in the High Plains. The surface soils of the ten ecoregions of Texas possess over 1,300 soil types.[11] Specific geologic units will characterize radon risk better than others, yet examination of only soil will fail to account for radon levels that accumulate in some home structure types and ventilation patterns.[12, 13] This study is the first follow-up to the original survey and utilizes indoor radon data collected over 12 years. The only radon study of the state was initiated in the early 1980s yielding low radon risk levels across the majority of the state and moderate risk levels in a portion of the Texas panhandle.[14] We report additional Texas regions with high-averaged indoor radon values. This data, when correlated with the underlying geology of Texas, suggests that buildings should be tested for indoor radon levels to remove uncertainty and limit the risk of adverse health outcomes causally linked to lung cancer from chronic radon inhalation.[15, 16]

ENVIRONMENTAL RADON: **SOURCES AND CLIMATIC CONDITIONS LEADING TO CONCENTRATION VARIATIONS**

Uranium is an element found in rock that decays through multiple spontaneous radioactive decay steps to radium (^{224}Ra), which decays to radon (^{222}Rn) gas.[17] Radon's decay products are also radioactive; emitting alpha and beta particles with short- and long-half-lives ranging from polonium's (^{214}Po)180 micro-seconds, to bismuth (^{210}Bi) in five days, to reach a stable lead isotope (^{206}Pb).[18] Radon gas, while naturally occurring, may accumulate to high levels indoors and become a health risk to the occupants. Protracted exposure to radon decay products has been causally linked to lung cancer. Each decay event emits ionizing alpha particles that may cause molecular cell damage, e.g., breaking base-pairs in DNA that disrupts protein production, which is a recognized contributor to cancerous mutations.[19-21] An individual's exposure risk to radiation is dependent on one's cumulative exposure; low cumulative exposure and rate increases lung cancer induction risk[22], which is increased in smokers.[23-25]

Uranium is present in soils worldwide and is geochemically classified as a lithophile, or 'rock-loving'. Uranium deposits are grouped by the International Atomic Energy Association (IAEA)[26, 27] into 15 major categories based on the host rock. Variable quantities of uranium may exist in rocks in various mineral assemblages. Some rocks have greater than 1 percent uranium concentrated in the stable form, triuranium octoxide (U_3O_8), which is considered high grade and economically profitable for mining.[28] Uranium distribution is not uniform in a rock or land area but may vary with soil thickness, grain size, and moisture content.

Several common rock types that contain uranium at above average crustal abundance include, sedimentary, granite, caliche, mudstone, limestone and alum shale.[26, 29, 30] A

review of several geological formations exposed across Texas that contain these rocks and their uranium abundances is summarized in Table 3.1. Few locations have the high ore-grades suitable for mining, however the Texas Coastal Plains, also known as South Texas Uranium Region or South Texas Mineral Belt, are considered the third largest sandstone-uranium hosted facies of rocks in the U.S.[31, 32] This uranium 'belt' consists of five uranium-bearing formations named the Goliad, Fleming and Oakville, Catahoula, Jackson Group, and Clairborne Group.[33] The Goliad Formation is predominantly filled with NW and SE faults.[34] These promote redistribution of dissolved uranium via groundwater flow.[35]

Table 3.1: Uranium-bearing soil and rock formations across Texas

Uranium-Bearing Formations	**County/Counties**	**Principal Soil that Hosts Uranium**
Lower Catahoula Formation[36]	Guadalupe, Gonzales, De Witt, Karnes, Wilson, Bee, Atascosa, McMullen, Live Oak, Goliad, La Salle, Frio	Sedimentary[37]
Eagle Ford Shale[38]	Guadalupe, Bee, Gonzales, De Witt, Karnes, Wilson, Atascosa, McMullen, Live Oak, Goliad, La Salle, Frio	Limerick mudstone, with clay and silt
Trans-Pecos[33]	Brewster, Culberson, El Paso, Hudspeth, Jeff Davis, Pecos, Presidio, Reeves, Terrell	Volcanic, sedimentary[33]
Fleming (Group), Oakville[31, 39] Formation	Karnes, Duval, Webb	Clay and coarse sedimentary[39]
Trujillo, Tecovas Formation	Armstrong	Sedimentary
Saul Ranch▪	Briscoe	Sedimentary
Nichols[40] *Tordilla Hill[39, 41]*	Karnes	Sedimentary Mudstone
Buzzard Draw[42]	Howard	Finchite mineral
Sulphur Springs[42]	Martin	Finchite mineral
**Jackson Group[43, 44]* Whitsett Formation	Karnes, McMullen, Duval, Live Oak[31]	Lignitic silt, sedimentary[37]
Kingsville Dome[31]	Kleberg	Coffinite Pitchblende
Goliad Formation[31]	Duval, Live Oak, Kleberg, Brooks, Goliad	Sandstone[33]
Hart-Mansfield▪, Saddleback Mesa,◊ Trujillo Camp◊	Oldham	Sedimentary, limestone
Mosure Ranch▪	Deaf Smith	Sedimentary

Table 3.1. Continued		
McArthur Ranch	Kent◊	Sedimentary
Sanderson, Swensen, Eubank, Long, Roddy Ranches, Caprock prospect	Garza▪	Sedimentary
Big Bend Exploration	Brewster▪	Limestone, sedimentary
Robinson Lease	Fayette▪	Siltstone
Chinle, Tecovas Formation	Borden◊	Limestone, claystone
Castle Mountain	Crane◊	Sedimentary, shale
Sand Creek Section	Crosby◊	Sedimentary, claystone
John Guitar Jr. Ranch	Dickens◊	Sedimentary, claystone
Lost Tubs Springs, Rotten Hill Fossil Quarry	Potter◊	Sedimentary, claystone
Palo Duro Canyon	Randall◊	Siltstone, sedimentary
Flat Top Mountain	Scurry◊	Claystone, sedimentary
W. Double Mountain	Stonewall◊	Claystone, limestone
Salinas, Kelsey Ranches	Starr▪	Sedimentary
Unnamed▪	Montague, Archer, Clay, Fisher, Wichita, Wilbarger	Sedimentary

*Important sediments of oil and gas reserves; oldest unit mined for uranium.
◊Information compiled and referenced from one USGS geologic survey (1967-1972).[45]
▪Information compiled and referenced from one USGS geologic survey (1943-1959).[46]

Texas has several extinct volcanoes , with many of them concentrated in the south and southwest of the state (Table 3.2), many of which, particularly along the line of the Rio Grande, are associated with significant mineralization and significantly higher than average uranium abundances. This underlying geology, coupled with fault structures associated with extension on the Ro Grand Rift, and locally diverse soil profiles are factors that may contribute to high radon levels in these regions.[47, 48]

Table 3.2: Several identified uranium-bearing volcanoes from North, Central and West Texas.			
Texas Volcano Name	**Mountain Range**	**Texas County**	**Host Rock Description**
Pilot Knob[49]	Not named	Travis; similar igneous rocks found in Uvalde	Volcanic, igneous[50]
Paisano[51]	Davis Mountain	Jeff Davis	Volcanic[52]
Sierra Quemada/Pine Canyon/ Tuff Canyon	Chisos ,Chinata, Christmas Mountains	Brewster and Presidio (Big Bend Nat Park)	Volcanic, fluorspar[52]
Trans-Pecos	Trans-Pecos Mountains Van Horn	Brewster, Culberson, El Paso, Hudspeth, Pecos, Jeff Davis, Reeves, Terrell	Volcanic, fluorite[52]
Eagle and Quitman ranges	Eagle Mountain Quitman Mountain[53]	Hudspeth	Volcanic, limestone[52]
Pedernales Falls	Not named	Blanco	Volcanic, limestone[54]

CONDITIONS SUITABLE FOR RADON TRANSPORT FROM SOIL: CLIMATE AND HOME FOUNDATIONS

Most residential homes in the U.S. are categorized by one of three structural foundation types and material quality: basement; crawlspace/pier and beam; slab.[55-57] Accordingly, several soil and climatic factors impact the emission dynamics and transport of radon into dwellings, and all exert strong control on persistent hazardous indoor air levels.[58] The variety and nonhomogeneous soil texture and porosity beneath the deep layers of a home's infrastructure permit radon permeation into homes through the slab foundation, cracks, expansion joints, plumbing, etc. Highly permeable soils below a home's foundation allows radon gas to easily travel horizontally and vertically through the soil profile.[59] Compact silt or clay soils are less permeable to radon gas; however, drought causes ground shrinkage and contraction shifts which produce fractures exposing the bedrock beneath and creates pathways along which radon gas may rapidly migrate to the soil surface.[60] Outdoor radon levels

correlate with soil types and tend to be higher in warm regions and arid soils. This is due to enhanced convective radon gas flow and outdoor air movements in different environments that may be seasonal.[61] These diverse soil and climatic controls, along with construction of energy-efficient homes with low outdoor air interchange rates, are more likely to lead to significant levels of indoor radon decay products.[62]

Radon infiltration into homes is driven by pressure differentials. Outside air will leak if there is a negative pressure difference (movement from high to low pressure). Temperature variations, such as warm air rising from furnaces, fireplaces, ovens, and stoves create pressure gradients. Warm air movement upward or through open chimneys, a thermal buoyancy also known as a 'stack effect'[63], will be replaced with colder air entering through existing gaps in the home's lower levels. Other forced air movements created by kitchen and bathroom exhaust fans, and even clothes dryer vents, will create similar pressure differences generating negative pressure zones (lower pressure than outside) on the home's foundation and ultimately the soil beneath the home. Additionally, weather episodes such as strong winds and stormy weather generate barometric pressure changes that lead to indoor radon level fluctuations.[64, 65]

INHALATION RISK OF RADON AND DECAY PRODUCTS TO THE RESPIRATORY TRACT

Lung tissue cells are sensitive to repeated assaults by a causative agent that can initiate inflammatory processes, cellular death, or irregular growth (cancer). These genetic changes overwhelm the body's repair mechanisms leading to genomic instability.[66-68] A latency period for lung cancer development depends on one's average inhalation dose and chronic exposure to radiation (radon products, prior tobacco smoking or passive tobacco smoke inhalation).[69] Lung cancer has the lowest survival rate and causes the highest proportion of

deaths in women.[23] To date, no specific medical test or symptom forewarns individuals to a gas that is odorless, tasteless, and unseen.[70]

The inhalation dose is dependent on the deposition amount to the respiratory tract. Use of a stochastic deposition model for assessing radon risk includes taking into account intra-subject physical exertion level, inhalation volume and the occupant's breathing pattern variations on aerosol deposition.[71] Increased breathing rate has been shown to decrease particle deposition in the upper lung tissue.[72] An individual man, woman, or child will have different inhalation rates and volumes, which leads to a heterogeneous exposure and hazard.[73] The health risk of inhaling radon progeny aerosols is most dependent on particle size deposition on lung tissue. Inhalable radioactive indoor particulate matter (PM), especially those sized less than 10 microns (10 μm) that settle into the deep fragile wall surface of the lungs' air sacs (alveoli), may permanently damage the impacted cells' performance or reproduction.[74, 75] An inhalation dose is not evenly distributed onto lung tissue and the precise number of lung cells affected is unknown in the course of living in a dwelling with high radon levels. For radioactive radon products to contribute to an oncogenic transformation, a multiple number of DNA cells on exposed tissue need to be affected by multiple alpha particle emissions.[76] Consequently, higher doses and longer exposures are more likely to cause DNA damage increasing the probability of manifesting to cancer.[77]

Inhalation of high radon levels in conjunction with tobacco smoke is more likely to generate non-small cell carcinoma, which is the lead cause for cancer deaths worldwide with an approximate 10% -16% survival rate at 5 years.[78] Between 80-90% of lung cancer are attributed to smoking.[79] The influence of radon exposure rate and cumulative exposure in the

majority (nearly 90%) of radon-induced lung cancers occurs in the smoker population.[76, 80-82] This leaves 10% of non-smokers diagnosed with lung cancer living in homes with low (< 74 Bq/m^3) and moderate (74 - 150 Bq/m^3) radon levels. A U.S. national health advisory regarding the dangers of high indoor radon was issued from the Office of the Surgeon General on January 13, 2005.[23, 48, 83] The U.S. National Academy of Science, by a charter granted from the U.S. Congress, appointed members to the National Research Council which published five reports (1972, 1980, 1990, 1999, 2005)[84] that informed the U.S. federal government on the carcinogenic effects of ionizing radiation. The *Biological Effects of Ionizing Radiation* (BEIR) reports have summarized the indoor radioactive hazards of the carcinogen radon.[85, 86] Published studies indicated that higher relative risks were associated with higher indoor radon levels. On the international level, committee research on radiation hazards is led by the United Nations Scientific Committee on the effects of Atomic Radiation (UNSCEAR), which is currently composed of scientists from 27 member states.[87] The 2006 UNSCEAR report concluded that a direct link to lung cancer risk from radon exposures in home exists.[88] The U.S. EPA estimates that 13.4 percent of lung cancer deaths of non-smokers are from exposure to indoor radon.[89]

CREATION OF THE FIRST U.S. EPA RADON MAP

The first and only EPA 'Map of Radon Zones' of the contiguous states was developed ca. 1990 (Figure 3.1) using data collected in the 1970s and early 1980s by the Department of Energy (DOE) National Uranium Resource Evaluation (NURE). Aerial radiometric surveys used a gamma-ray spectrometer mounted on an aircraft that traveled 122 m above the ground, patterned using 2 - 10 km flight line spacing. At a typical aerial speed of 70 knots a distance of

approximately 118 feet is travelled in one second.[90] This resulted in mapping the equivalent uranium (eU) across the U.S.; equivalent uranium corresponds to 1.76 MeV (mega-electron volts) of bismuth-214 (^{214}Bi).[14] A drawback to using this equipment is that gamma rays lose radiation intensity with increasing distance from the terrestrial source and is attenuated by water presence.[91] This spectrometry is also subject to other environmental interference factors, such as clouds and ground vegetation.[92]

Other data used in mapping included indoor radon levels of approximately 100,000 homes nationwide; 1200 homes in Texas were tested.[14] The low-level (Zone 3) was defined as <74 Bq/m^3, the mid-level (Zone 2) was defined as 74 - 111 Bq/m^3, and the high-levels (Zone 1) defined as >150 Bq/m^3 or more of radon. The use of county demarcation for radon averages within states evades the bedrock variety that exists beneath our homes in smaller localities. Due to the outdated source map, some home owners have referenced the map to justify whether their residential county necessitated radon testing. Yet, EPA's statement accompanying the map insisted homeowners overlook the county boundaries and recommended that each home be tested for radon for accurate personal dwelling risk estimation.[93]

This survey coverage equated to <10% of the U.S. and the airborne gamma-ray detectors detect emission within 20-30 cm of the surface (just below the organic layer or the A horizon). In the B horizon is any weathered uranium material from the parent-ore-rock layers in the C horizon. Due to the depth differences between the B and C horizons, along with the depth-limit for gamma ray detection, the aerial surface detectors are expected to underestimate the actual geologic soil gamma radiation.[14]

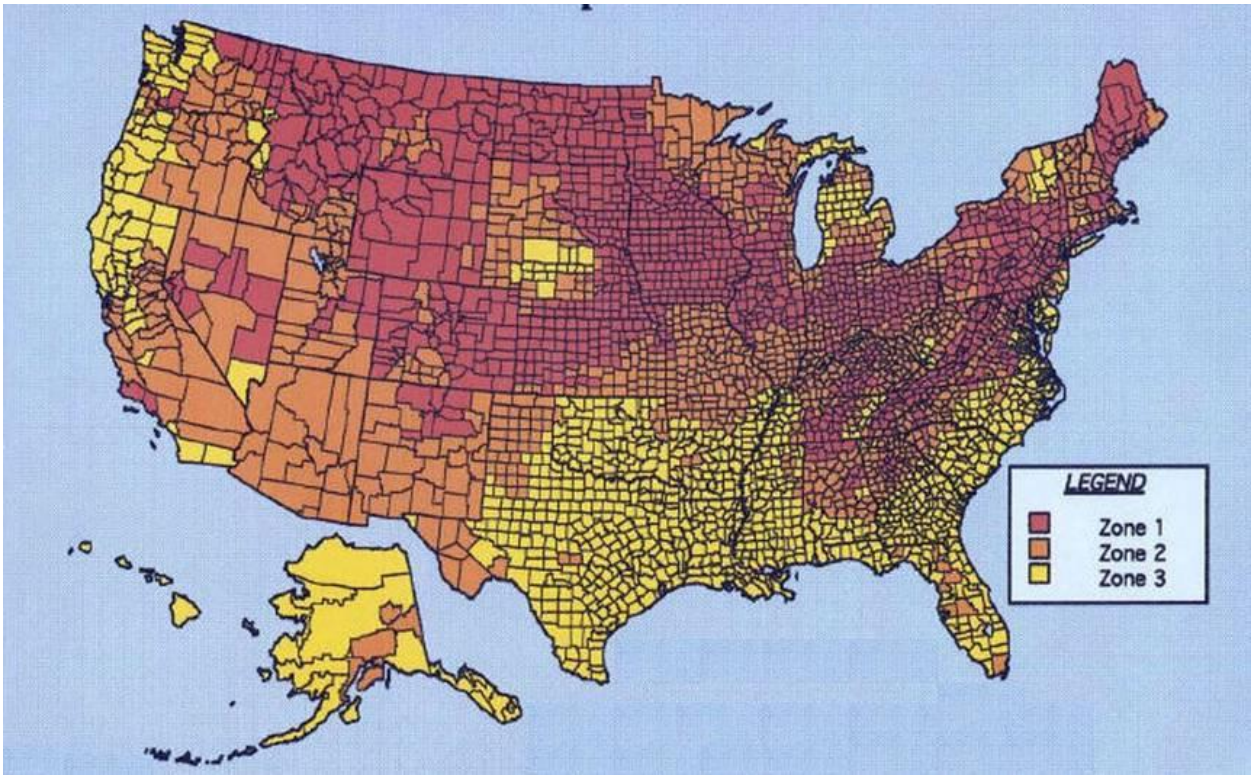

Figure 3.1: First EPA map created circa 1990. https://www.epa.gov/sites/production/files/2015-07/documents/zonemapcolor.pdf; accessed 10 July, 2018.

INDOOR RADON TESTS

AVERAGED DATA FROM TESTING LABORATORY

Data was tabulated from home test kits analyzed by Alpha Energy Laboratory in Carrollton, TX. [The lab is certified by the American Association of Radon Scientists and Technologists (AARST) under the National Radon Proficiency Program (NRPP); certification number 101132AL.] Residential addresses of all test results received from the laboratory were geocoded blind so that no home could be specifically located. The data was grouped by county and by zip code to

create the averaged indoor radon levels for the mapping using the ESRI 2017, ArcGIS Desktop package, Redlands, CA; Environmental Systems Research Institute.

Laboratory background measurement results were annotated on each passive sample analysis, along with temperature, humidity, air flow, and any concentration changes in the analysis. Equipment calibration was determined by the analytical instrument response to a traceable radon decay product with known concentration and derived from a certified NIST ^{226}Radium-standard. There is no Standard Reference Material (SRM) for ^{222}Rn. The Lower Limit of Detection (LLD) was determined during each test day, calculated from the laboratory background measurements, which change overtime.

The user was asked to describe the foundation type of the facility tested, yet many of these users left this area blank. The main types listed were slab, and pier and beam. The difference in radon levels between these foundation types was not made in this study. For this printing, the test dates ranged from Mar 2001 to 9 Jun 2018. (Repeat tests are not identified by the homeowner or tracked by the receiving lab.)

CURRENT STUDY FOR TEXAS MAP UPDATE

In the current study, both activated charcoal and alpha track kits were analyzed by Alpha Energy Laboratories, Inc., Carrollton, Texas, after home testing for 2-4 days and >91-365 days, respectively. Data from greater than 28,500 Texas homes in 217 Texas counties were compiled to yield the averaged county readings. 81 counties (32%) returned ten or greater home test kits to produce the current color-coded state map, Figure 3.2. To date, 37 counties (15%) have no homes tested using this testing laboratory. Of the 217 counties tested, 34 counties (16%) have indoor radon levels categorized as Zone 1, which are indoor radon levels >150 Bq/m^3.

Previously no counties (0%) were described as Zone 1. The color-coding scheme remains the same to the 1990 EPA Texas Indoor Radon map.

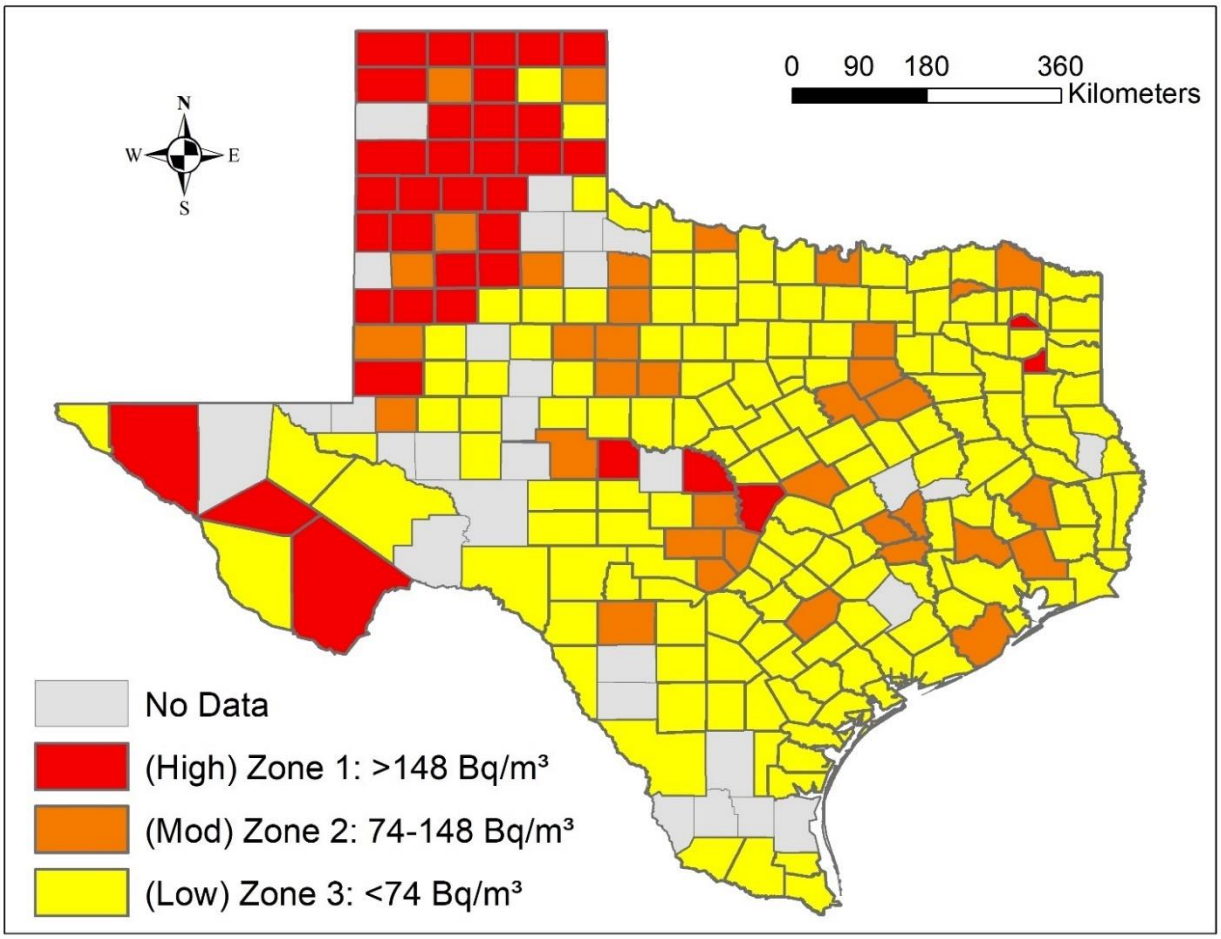

Figure 3.2: The map is constructed into color-coded "Zones 1-3" according to the averaged data points in the Texas counties with equal to or greater than 5 (n ≥5) tested homes. Areas shaded in gray have insufficient data (less than 5 data points) to average for the county radon potential.

Since county boundaries are created for political and administrative purposes, and not by land geology, the Zone 1, high potential indoor radon levels tested in zip coded areas are shown with an overlay on the averaged Zone 3, Low potential counties. This zip coded-map design

more closely resembles the diverse province geology (Figure 3.3) of the regions versus county line demarcation. It also brought test evidence that 41 counties, with an averaged indoor data < 74 Bq/m^3 (Low potential, Zone 3) on the updated map, consist of homes in zip codes which tested with indoor radon levels greater than 150 Bq/m^3 (High potential, Zone 1).

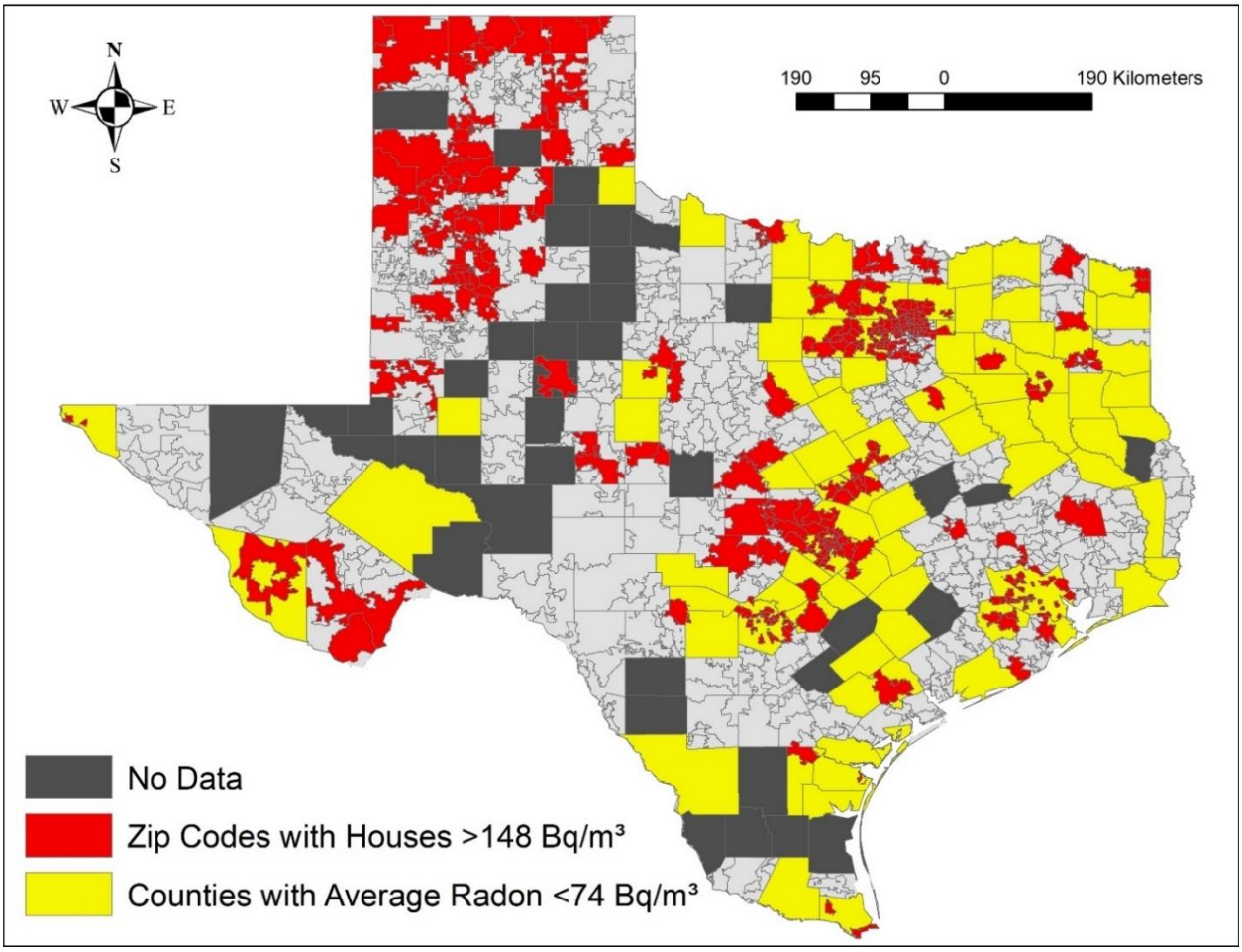

Figure 3.3: The map is constructed to show the low level areas (yellow) with zip codes that have tested with high (red) indoor radon test levels. Additionally, zip codes within areas that tested with average indoor radon levels in moderate to high levels are included.

EUROPEAN UNION, INTERNATIONAL ATOMIC ENERGY AGENCY, AND THE U. S.

The European Union (EU) with the joint support of the International Atomic Energy Agency (IAEA) and World Health Organization (WHO), submitted a "Basic Safety Standards (BSS) Directive", Council Directive 2013/59/Euratom[94, 95], defining maximum permissible radon exposure levels to workers and the public. [Euratom is the European Atomic Energy Community[96]] The EU member states developed a regulatory policy to actively reduce radon exposure in occupational and public settings to an annual average concentration in air set to a maximum of 300 Bq/m^3.[97] The BSS directive enforces building codes and other construction guidelines for safety standards across all EU member states.

The U.S. has a patchwork of laws governing indoor exposure testing and mitigation plans to dwellings with radon levels exceeding the EPA action level. Indoor air quality management has been established for low-income housing under the authority of the U. S. Department of Housing and Urban Development (HUD). Since the 2013 policy was established, all mortgage insurance for new multifamily housing lenders under the Federal Housing Administration (FHA) are required to provide a radon test report.[98] If new construction in 'high-radon risk areas' is not built using radon resistant methods[99] a mitigation plan is required to meet FHA application acceptance. The updated map will now require this to be performed in several Texas regions. Color-coding by zip code (Figure 3.3) is an alternative way to emphasize the existence of elevated radon levels in areas that may be averaged as low radon concentrations using larger county demarcations. Smaller area characterizations of soil geology will improve characterizing/delineating radon level anomalies in county-sized regions. Oversight of local standards can be delegated to individual cities, with periodic inspection of compliance performed by Radiation Safety Officers (RSO) in the state who are trained representatives of the

Nuclear Regulatory Commission (NRC) standards for indoor radiation protection. RSO training would include education on radon test devices, incurred risks from radiation exposure, contamination prevention, and up-to-date radon mitigation designs. Another eligible network of testers are healthcare workers that visit rural areas and homes of financially impoverished families.

DISCUSSION

The state of Texas consists of 254 counties of various sizes and populations. Within the data surveyed, 42 Texas counties tested with radon levels between 148 to 342 Bq/m^3, which yielded indoor radon test result averages ≥150 Bq/m^3, which surpasses the EPA recommended action level to improve indoor air quality. The top four largest tested areas during the 12-year study period of were received from Dallas, Travis, Tarrant and Harris Counties, respectively. The lung and bronchus (L&B, age-adjusted) cancer incidence increased by county population size, but not consistently. The Texas county L&B similarly increased with an increase in average tested indoor radon concentrations, but not consistently across the state. Home survey paperwork did not consistently annotate the home foundation type to yield a summarization of zip codes to ground support materials.

With the projected population increase in several counties (Table 3.3) which tested with above average county values and exceeding the EPA action level, builders and realtors have a responsibility to educate the public of the dangers of chronic and high indoor radon levels. Although the number of tested homes in this study is larger than previously used in the creation of a Texas radon map, some counties are under-represented in zip codes area (Table 3.4) and others without any data for area evaluation (Figure 3.3, 14.6%). To increase coverage of the

state zip codes and counties activated charcoal kits were distributed at no charge to participants at local realtor shows, offerings through Texas Tech University electronic mail to faculty, staff and students, and public retail establishments to those counties with no testing data from Alpha Energy Laboratories, Inc. Calls to distant county public health departments were also made requesting distribution to willing area residents, preferably with slab foundations.

The U.S. EPA has consistently recommended that all homes, in all zones, be tested for indoor radon. General conclusions of indoor radon levels deduced by the survey of individual homes and relating it to the geology is the favored technique. An accurate mapping of indoor radon potential is dependent on local soil geology, variation in the distribution of heterogeneous soil porosity and texture, the meteorological conditions, climate, temperature and moisture at test time, the building construction material, ventilation and air exchange. An analysis of the interplay of regional geography and climate changes will support mitigation measures and the management of indoor radon and the decay product accumulation.[100] Home testing approaches include several test time lengths, lab-tested kits or continuous monitoring devices with measurements displayed. This personal empirical experimentation and observation will help quantify the risk posed within a dwelling.

Table 3.3: Texas counties with a wide range of population sizes. The table of counties is listed in order of increasing averaged indoor radon levels. This increased tabulated trend nearly follows the increasing lung and bronchus cancer incidence, from 2011 through 2015, in the selected counties.

TX County	**[Rn Average] (Bq/m^3)**	**Age-Adjusted L&B Incidence Rate per 100,000**	**(Bq/m^3) Highest Level Tested**	**Population Apr, 2010↗**	**Population Projected to July, 2017**	**Total Area mi^2 ⁘**
Bexar	37	(↓) 42.4	3,700	1,722,797	+14.2%	1256
Travis	37	(↑) 43.2	392	1,030,522	+19.7%	1023
Harris	37	(↓) 50.9	237	4,107,854	+13.7%	1777
Harrison	52	(↓) 72.8	189	65,752	+1.0%	916
Dallas	74	(↓) 52.7	291,523	2,372,257	+10.6%	909
Gillespie	74	(↓) **36.2**	1,380	24,885	+7.3%	1062
Tarrant	74	(↓) 57.5	792	1,817,417	+13.5%	902
Montgomery	81	(↓) **56.4**	12,987	459,185	+25.3%	1077
Llano	111	(↑) 57.5	403	19,332	+9.9%	966
Lubbock	237	(↓) **52.5**	5,550	280,286	+9.4%	901
Lamb	318	(↓) **39.1**	396	13,993	-5.5%	1018
Brewster	326	(↓) **39.9**	1,473	9,260	+1.1%	6192
Tom Green	385	57.0	21,460	110,677	+7.1%	1541
Burnet	444	61.3	3,793	42,755	+9.6%	1021

L&B = lung and bronchus; * State 2011-2015; all races, both sexes, all ages. (↓ or ↑) Recent **5-yr trend** in Incidence Rates; no marking indicates no change; accessed July 9, 2018. (https://statecancerprofiles.cancer.gov/incidencerates/index.php?stateFIPS=48&cancer=047&race=00&sex=0&age=001&type=incd);

↗ https://www.tsl.texas.gov/ref/abouttx/popcnty201011.html; accessed July 9, 2018

⁘ http://www.texascounties.net/statistics/landarea.htm; accessed July 9, 2018

Table 3.4: Counties arranged by increasing lung and bronchus incidence. A sample of northern (N), southern (S), and central (C) counties selected for comparison of increasing averaged indoor radon concentrations.

County	**L&B**	**[Rn] avg Bq/m^3**	**Population***	**Rn data pts**	**Zip code: #tested/#total**	**Texas U area quadrant**
Bexar	42.4	37	1,898,000	1,171	50/104	(**S**) S. Central Coastal Plain
Gillespie	36.2	74	25,963	19	1/5	(**C**) Edwards (limestone) Hill country
Lamb	39.1	318	13,385	5	4/8	(**N**) South Plains
Brewster	39.9	326	9,145	40	2/6	(**W**) Big Bend (limestone)[101]
Tom Green	57.0	385	118,105	84	6/19	**W**. Central (C) San Angelo Formation
Burnet[102]	61.3	363	45,463	35	3/10	(**C**) Marble Falls Limestone[103]
Angelina	70.9	37	88,255	22	5/9	**E**astern TX near Louisiana
Red River	76.6	148	12,455	6	3/6	**NE** borders Oklahoma

L&B: Age-Adjusted L&B Incidence Rate per 100,000; * State 2011-2015; all races, both sexes, all ages

*****U.S. Census Bureau, 2015; accessed September 19, 2018.

To modify and improve indoor air quality we must evaluate the existing radon risk levels by testing multiple days and within different living areas, e.g. basement, attic, second floor, etc. Determining indoor occupancy exposure, to evaluate the radon risk, varies from dwelling to dwelling, day to day, and within populations (smokers, genetics, etc.). It is these variabilities that lead to limitations in accurately quantifying lung cancer deaths from the inhalation of indoor radon's radioactive products. In addition, a conclusive relationship relies on linking a 'cancer-formation years in the making' to an immune function downfall or DNA chemical break that led to a production error and tumor. As with any NORM ionizing radiation on biological cells, the damage to DNA from protracted radiation exposure exceeds our body's repair

limitations; overt symptoms are lacking until the cancer befalls us. Evaluating the radon risk through a home test is an essential first step in removing the uncertainty factor in the indoor air quality.

CONCLUSION

Radon exists in Texas at various levels and is expected due to the ubiquitous presence of uranium in the underlying rock (geology) of the State. A strong causal relationship between radon exposure and lung cancer risk exists, an especially heightened synergism for smokers. Radon presence is not delineated or accurately represented by county lines nor county-averaged measurements. Despite these mapping shortcomings, predictions using zip codes correlated with geology is potentially a more predictive measure of radon levels in the vast and diverse regions of Texas. Bringing attention to the newly mapped Texas 'regions' would provide awareness to individuals livings in radon prone areas of a possible risk. This study provided an appropriate update to approach state regulatory policies in home construction material use and mitigation installation into pre-built homes. Building assessments performed by certified professionals are important first steps in indoor air quality management yielding real-time radon levels. The goal is to educate the community on indoor home air quality to minimize the long-term radon product exposure.

ACKNOWLEDGMENTS

The authors thank Naveen Kumar for technical assistance in statistical improvements and Owen Reese, Business Director of Alpha Energy Laboratories for access to anonymized Texas county data.

FUNDING

This work was supported by the Environmental Protection Agency Grant No. 00F94602.

REFERENCES

1. EPA, *User's Guide: Radionuclide Carcinogenicity.* 2015.
2. *Toxic Substances Control Act*. 2017, U.S. Government: Washington, DC. p. 154.
3. EPA. *Radiation Protection: Radiation Sources and Doses*. 2017 [cited 2018 February 23, 2018]; Available from: https://19january2017snapshot.epa.gov/radiation/radiation-sources-and-doses_.html.
4. EPA, *Radionuclides (Including Radon, Radium and Uranium); Hazard Summary*, (IRIS), Editor. 2000, EPA: Washington, C.C. p. 1-5.
5. Kim, S.-H., et al, *Attributable Risk of Lung Cancer Deaths Due to Indoor Radon Exposure.* Annals of Occupational and Environmental Medicine, 2016. **28**(8): p. 1-7.
6. Samet, J.M., et al, *Lung Cancer in Never Smokers: Clinical Epidemiology and Environmental Risk Factors.* Clinical Cancer Research, 2009. **15**(18): p. 5626-5645.
7. Thun, M.J., et al, *Lung Cancer Death Rates in Lifelong Nonsmokers.* Journal of the National Cancer Institute, 2006. **98**(10): p. 691-699.
8. Sethi, T.K., et al, *Radon and Lung Cancer.* Clinical Advances in Hematology & Oncology, 2012. **10**(3): p. 157-164.
9. Plocheck, R., ed. *Texas Almanac (2010–2011 ed.).* 2000-2011 ed. 2011.
10. Bomar, G.W. Handbook of Texas Online, George W. Bomar, "WEATHER," accessed September 21, 2018, http://www.tshaonline.org/handbook/online/articles/yzw01. 2010 June 15, 2010 [cited 2018 September 21, 2018]; Texas State Historical Society]. Available from: https://tshaonline.org/handbook/online/articles/yzw01.
11. USDA. *General Soil Map of Texas*. Texas Soil Survey 2008 [cited 2018 October 10, 2018]; Available from: http://texasalmanac.com/topics/environment/soils-texas.
12. EPA, *Building Radon Out: A Step-by-Step Guide On How To Build Radon-Resistant Homes*. 2001. p. 84.
13. Darby, S.C., et al, *Radon in Homes and Risk of Lung Cancer: Collaborative Analysis of Individual Data from 13 European Case-Control Studies.* The BMJ, 2004.
14. EPA, *EPA's Map of Radon Zones: Texas*. 1993: Washington, D.C. p. 88.
15. Axelsson, G., et al, *Lung Cancer Risk From Radon Exposure In Dwellings In Sweden: How Many Cases Can Be Prevented If Radon Levels Are Lowered?* Cancer Causes & Control, 2015. **26**(4): p. 541-547.
16. Choi, J.R., et al, *Novel Associations Between Lung Cancer-Related Genes and Indoor Radon Exposure.* Journal of Cancer Prevention, 2017. **22**(4): p. S449.
17. *Radon Decay Products in the Atmosphere*, in *Radon in the Environment*, M. Wilkening, Editor. 1990, Elsevier. p. 81-90.
18. Hopke, P.K., *Radon and Its Decay Products*, in *ACS Symposium Series*. 1987, American Chemical Society. p. 628.
19. Han, W., et al *Ionizing Radiation, DNA Double Strand Break and Mutation*, in *Advances in Genetics Research*, K.V. Urbano, Editor. 2010, Nova Science Publishers, Inc. p. 1-13.
20. Martin, L., et al, *DNA Mismatch Repair and the DNA Damage Response To Ionizing Radiation: Making Sense of Apparently Conflicting Data.* Cancer Treatment Reviews, 2010. **36**(7): p. 518-527.
21. Spitz, M.R., et al, *Genetic Susceptibility to Lung Cancer: The Role of DNA Damage and Repair.* Cancer Epidemiology, BioMarkers and Prevention, 2003. **12**: p. 689-698.

22. NRC, *Health Risks of Radon and Other Internally Deposited Alpha Emitters*, in *Biological Effects of Ionizing Radiations: BEIR IV*, NRC, Editor. 1988, National Academies Press (US): Washington, D.C.
23. EPA. *Exposure to Radon Causes Lung Cancer In Non-smokers and Smokers Alike*. Health Risk of Radon 2018 [cited 2018 April 7, 2018]; Available from: https://www.epa.gov/radon/health-risk-radon.
24. Lantz, P.M., et al, *Radon, Smoking, and Lung Cancer: The Need to Refocus Radon Control Policy.* American Journal of Public Health, 2013. **103**(3): p. 443-447.
25. Leuraud, K., et al, *Radon, Smoking and Lung Cancer Risk: Results of a Joint Analysis of Three European Case-Control Studies Among Uranium Miners.* Radiation Research, 2011. **176**: p. 375-387.
26. WNA. *Geology of Uranium Deposits*. 2015 February, 2015 [cited 2018 February 5, 2018]; Available from: http://www.world-nuclear.org/information-library/nuclear-fuel-cycle/uranium-resources/geology-of-uranium-deposits.aspx.
27. IAEA, *Uranium 2014: Resources, Production and Demand (The Red Book)*. 25 ed. 2014.
28. IAEA, *Methods of Exploitation of Different Types of Uranium Deposits*. 2000: Vienna, Austria. p. 84.
29. Lewan, M.D., Buchardt, B., *Irradiation of Organic Matter by Uranium Decay in the Alum Shale, Sweden.* Geochemica et Cosmochimica Acta, 1989. **53**(6): p. 1307-1322.
30. Swanson, V.E., *Geology and Geochemistry of Uranium in Marine Black Shales A Review*, in *Uranium in Carbonaceous Rocks*. U.S. Atomic Energy Commission: Washington 25, D.C. p. 1-51.
31. *Texas Coastal Plain Uranium Region*, in *Uranium Deposits of the World: USA and Latin America*, F.J. Dahlkamp, Editor. 2010, Springer: Bonn, Germany. p. 311-355.
32. USGS, *Assessment of Undiscovered Sandstone-Hosted Uranium Resources in the Texas Coastal Plain, 2015.* 2015.
33. Sass, R.L., *Uranium Mining in Texas: Why is it Done That Way?* 2011.
34. Dahlkamp, F.J., *Texas Coastal Plain Uranium Region*, in *Uranium Deposits of the World*, F.J. Dahlkamp, Editor. 2010.
35. Page, L.R., *Guides to Prospecting for Uranium and Thorium in New Hampshire and Adjacent Areas*, in *United States Department of the Interior Geological Survey*. 1980. p. 25.
36. Ledger, E.B., et al, *An Evaluation of the Catahoula Formation as a Uranium Source Rock in East Texas*, in *Gulf Coast Association of Geological Societies Transactions*. 1984, American Association of Petroleum Geologists. p. 99-108.
37. Houser, B.B., *Geology and Mineral Resource Potential Map of the Graham Creek Roadless Area, Angelina and Jasper Counties, Texas*, USGS, Editor. 1983.
38. Breyer, J.A., et al. *Facies, Fractures, Pressure and Production in the Eagle Ford Shale (Cretaceous) between the Maverick Basin and the San Marcos Arch, Texas, USA*. in *Unconventional Resources Technology Conference*. 2013. Denver, CO.
39. Esaka, F., et al, *Dependence of the Precision of Uranium Isotope Ratio on Particle Diameter in individual Particle Analysis With SIMS.* Applied Surface Science, 2008. **255**: p. 1512-1515.

40. UEC. *Uranium Energy News Releases*. News & Media 2008 [cited 2018 May 2, 2018]; Available from: http://www.uraniumenergy.com/news/releases/2008/index.php?content_id=290.
41. Bunker, C.M., et al, *Geology of the Oxidized Uranium Ore Deposits of the Tordilla Hill-Deweesville Area, Karnes County Texas: A Study of a District Before Mining*. 1973: Washington, D.C. p. 46.
42. Hawes, T., *USGS: Uranium Has Been Found Near Big Spring*. 2017, Midland Reporter-Telegram.
43. USGS, *Sedimentary Depositional Environments of Uranium and Petroleum Host Rocks of the Jackson Group, South Texas.* Journal of Research of the U.S. Geological Survey, 1976. **4**(5): p. 615-629.
44. Dickinson, K.A., *Uranium and Thorium Distribution in Soils and Weathered Bedrock in South Texas*. 1977.
45. Finch, W.I., et al, *Measured Strati Graphic Sections of Uranium-Bearing Upper Triassic Rocks of the Dockum Basin, Eastern New Mexico, West Texas, and the Oklahoma Panhandle With Brief Discussion of Stratigraphic Problems*, USGS, Editor. 1983.
46. Finch, W.I., *Geology of Epigenetic Uranium Deposits in Sandstone in the United States*, in *Geological Survey Professional Paper*. 1967, USGS: Washington, DC. p. 128.
47. Bruno, R.C., *Sources of Indoor Radon in Houses: A Review.* Journal of the Air Pollution Control Association, 1983. **33**(2): p. 105-109.
48. EPA, *Home Buyer's and Seller's Guide to Radon*, in *Indoor Air Quality*. 2013, U.S. EPA. p. 1-44.
49. King, R.R., et al, *Geological Survey Bulletin, Issue 4; Issue 1195*, in *Bibiography of North American Geology, 1950-1959*. USGS. p. 3796.
50. Long, L. *Looking Back at the Life of Austin's Once-Explosive Volcano, Pilot Knob*. 2015 [cited 2018 June 6, 2018]; Available from: https://www.jsg.utexas.edu/news/2015/11/looking-back-at-the-life-of-austins-once-explosive-volcano-pilot-knob/.
51. Parker, D., et al, *Large-Scale Alkalic Magmatism Associated With the Buckhorn Caldera, Trans-Pecos Texas, USA: Comparison with Pantelleria, Italy.* Bulletin of Volcanology, 2008. **70**: p. 403-415.
52. Henry, D.a. *Uranium Deposits in Volcanic Rocks*. in *Proceedings of a Technical Committee Meeting*. 1985. El Paso, TX: IAEA.
53. Murray, D.H., *Mineralization in the Northern Quitman Mountains, Hudspeth County, Texas*, in *New Mexico Geological Society Guidebook, 31st Field Conference, Trans-Pecos Region, 1980*. 1980. p. 267-270.
54. USGS. *The History of Texas is Under Your Feet and at Your Fingertips!* 2015 [cited 2018 October 10, 2018]; Available from: https://www.usgs.gov/news/history-texas-under-your-feet-and-your-fingertips.
55. Laquatra, J., et al, *Housing Technology in the United States.* Housing and Society, 1992. **19**(2): p. 41-55.
56. Quikrete.com. *Concrete Foundations*. Available from: https://www.quikrete.com/espanol/pdfs/projects/concretefoundations.pdf.

57. PermaPier. *The Three Types of Home Foundation Design*. 2015 May 25, 2015 [cited 2018 September 19, 2018]; Available from: https://www.permapier.com/blog/the-three-types-of-home-foundation-design/.
58. Mose, D.G., et al, *Reliability of Inexpensive Charcoal and Alpha-Track Radon Monitors.* Natural Hazards, 1990. **3**: p. 341-355.
59. Szabo, K.Z., et al, *Dynamics of Soil Gas Radon Concentration in a Highly Permeable Soil Based On a Long-Term High Temporal Resolution Observation Series.* Journal of Environmental Radioactivity, 2013. **124**: p. 74-8.
60. Moreno, V., et al, *Soil Radon Dynamics in the Amer Fault Zone: An Example of Very High Seasonal Variations.* Journal of Environmental Radioactivity, 2016. **151**: p. 293-303.
61. Arvela, H., et al, *Effect Of Soil Moisture On Seasonal Variation In Indoor Radon Concentration: Modelling And Measurements In 326 Finnish Houses.* Radiation Protection Dosimetry, 2016. **168**(2): p. 277-290.
62. Fleischer, R.L., et al, *Indoor radon levels: Effects of energy-efficiency in homes.* Environment International, 1982. **8**(1-6): p. 105-109.
63. Parra, J.P., et al, *Natural Ventilation of Parral Greenhouses.* Biosystems Engineering, 2004. **87**(3): p. 355-366.
64. Jonassen, N., *On the Effect of Atmospheric Pressure Variations on the Radon-222 Concentration in Unventilated Rooms.* Health Physics, 1975. **29**(1): p. 216-220.
65. Tchorz-Trzeciakiewicz, D.E., Klos, M., *Factors Affecting Atmospheric Radon Concentration, Human Health.* Science of The Total Environment, 2017. **584-585**: p. 911-920.
66. Howard, J., *Minimum Latency & Types of Categories of Cancer*. 2015.
67. Schaue, K., et al, *Cytokines in Radiobiological Responses: A Review.* Radiation Research, 2012. **178**(6): p. 505-523.
68. Colotta, F., et al., *Cancer-Related Inflammation, the Seventh Hallmark Of Cancer: Links To Genetic Instability.* Carcinogenesis, 2009. **30**(7): p. 1073-1081.
69. Archer, V.E., et al, *Latency and the Lung Cancer Epidemic Among United States Uranium Miners.* Health Physics, 2004. **87**(5): p. 480-489.
70. HHS, *Surgeon General Releases National Health Advisory On Radon*. 2005, HHS Press Office: Surgeon General's Workshop on Healthy Indoor Environment. p. 1-2.
71. Koblinger, L., *Analysis of Human Lung Morphometric Data For Stochastic Aerosol Deposition Calculations.* Physics in Medicine & Biology, 1985. **30**(6): p. 541.
72. Mohamed, A., et al, *Deposition Pattern of Inhaled Radon Progeny Size Distribution in Human Lung.* Journal of Radiation Research and Applied Sciences, 2014. **7**: p. 333-337.
73. EPA, *Inhalation Rates*, in *Exposure Factors Handbook*. 2011. p. 1-96.
74. EPA. *Particulate Matter (PM) Basics*. Particulate Matter (PM) Basics 2016 September 12, 2016 [cited 2018 March 30, 2018]; Available from: https://www.epa.gov/pm-pollution/particulate-matter-pm-basics.
75. Coggle, J.E., et al, *Radiation Effects in the Lung.* Environmental Health Perspectives, 1986. **70**: p. 261-291.
76. Monchaux, G., et al, *Influence of Exposure Rate on Lung Cancer Induction in Rats Exposed to Radon Progeny.* Radiation Research, 1999. **152**: p. S137-S140.
77. Robertson, A., et al, *The Cellular and Molecular Carcinogenic Effects of Radon Exposure: A Review.* International Journal of Molecular Science, 2013. **14**(7): p. 14024-14063.

78. Choi, J.R., et al, *Gene Mutation Discovery Research of Non-Smoking Lung Cancer Patients Due to Indoor Radon Exposure.* Annals of Occupational and Environtal Medicine, 2016. **28**(13): p. 6.
79. Fenelon, A., et al, *Estimating Smoking-Attributable Mortality in the United States.* Demography, 2012. **49**(3).
80. Association, A.L. *What Causes Lung Cancer?* 2017 November 27, 2017 [cited 2018 January 16]; Available from: http://www.lung.org/lung-health-and-diseases/lung-disease-lookup/lung-cancer/learn-about-lung-cancer/what-is-lung-cancer/what-causes-lung-cancer.html?referrer=https://www.google.com/.
81. Cancer.Gov. *Radon and Cancer*. Cancer-Causing Substances 2011 December 6, 2011 [cited 2018 July 5, 2018]; Available from: https://www.cancer.gov/about-cancer/causes-prevention/risk/substances/radon/radon-fact-sheet.
82. ICRP, *Protections Against Radon-222 at Home and at Work*, in *Annals of the ICRP: The 2007 Recommendations of the International Commission On Radiological Protection*, J. Valentin, Editor. 2007. p. 34.
83. EPA, *A Citizen's Guide to Radon The Guide to Protecting Yourself and Your Family from Radon*. 2012: Washington, D.C. p. 1-16.
84. NRC, *Committee On the Biological Effects of Ionizing Radiations*. 1990, National Academies Press: Washington, D.C. p. 493.
85. NRC, *Health Effects of Exposure to Radon: BEIR VI*. 1999, National Academy Press: Washington, D.C. p. 1-593.
86. NRC, *Health Risks from Exposure to Low Levels of Ionizing Radiation: BEIR VII Phase 2*. 2006, The National Academies Press: Washington, D.C. p. 422.
87. UNSCEAR. *United Nations General Assembly*. 2017 16 August 2017 [cited 2018 April 7, 2018]; Available from: http://www.unscear.org/unscear/en/about_us/memberstates.html.
88. UNSCEAR, *Effects of Ionizing Radiation: United Nations Scientific Committee on the Effects of Atomic Radiation*. 2006: New York, NY. p. 338.
89. EPA, *EPA Assessment of Risks From Radon in Homes*. 2003: Washington, D.C. 20460.
90. *Technical Capability Standard for Aerial Mounted Radiation Detection Systems*. 2017, Domestic Nuclear Detection Office (DNDO). p. 45.
91. Wilford, J.R., et al, *Application of airborne Gamma-Ray Spectrometry in Soivregolith Mapping and Applied Geomorphology.* Journal of Australian Geology & Geophysics, 1997. **17**(2): p. 201-216.
92. Mahmood, H.S., et al, *Proximal Gamma-Ray Spectroscopy to Predict Soil Properties Using Windows and Full-Spectrum Analysis Methods.* Sensors, 2013. **13**(12): p. 16263-16280.
93. EPA, *EPA Map of Radon Zones*. 2015.
94. Bochicchio, F., *Protection From Radon Exposure at Home and at Work in the Directive 2013/59/Euratom.* Radiation Protection and Dosimetry, 2014: p. 1-6.
95. ERA. *Improving Awareness and Reducing Risk of Radon Exposure Across Europe*. 2014 [cited 2018 April 23, 2018]; Available from: http://radoneurope.org/index.php/activities-and-events-2/working-groups/radon-regulation/.
96. EU, *Council Directive 2013/59/Euratom*, in *Non-Legislative Acts*. 2014. p. 73.

97. *JRC Conference and Workshop Reports*. in *2nd International Workshop on the European Atlas of Natural Radiation*. 2017. Verbania, Italy.
98. HUD, *HUD Office of Multifamily Development Radon Policy*. 2013: Washington, D. C. p. 1-7.
99. EPA. *Building Codes for Radon-Resistant New Construction (RRNC)*. Radon 2009 August 10, 2017 [cited 2017 August 30, 2017]; Available from: https://www.epa.gov/radon/building-codes-radon-resistant-new-construction-rrnc#states.
100. Chen, C., et al, *Modeling of Radon Transport in Unsaturated Soil.* Journal of Geophysical Research, 1995. **100**(B8): p. 15517-15525.
101. Eargle, D.H., *Some Uranium Occurrences in West Texas*, in *Trace Elements Investigations Report 574*, USGS, Editor. 1956. p. 32.
102. White, D.M., et al, *Information and Statistical Facts on Coal and Uranium Mining in Texas*, in *Energy Resource Comparisons*, M.B. Hodgkiss, Editor. 1991, Railroad Commission of Texas: Austin, TX. p. 62.
103. Petrossian, R., et al, *Economic Geology Resources of the Llano Uplift Region and the Historical Impacts to the Region's Growth*. 2016. p. 71.